Bulletin of the Geological Survey of Japan, vol.58 (9/10), p. 323- 350 , 2007

Chemical compositions of the late Cretaceous Ryoke granitoids of the Chubu District, central Japan – Revisited

Shunso Ishihara[1] and Bruce W. Chappell[2]

Shunso Ishihara and Bruce W. Chappell (2007) Chemical compositions of the late Cretaceous Ryoke granitoids of the Chubu District, central Japan – Revisited. *Bull. Geol. Surv. Japan*, vol. 58 (9/10), 323-350, 15 figs, 4 tables, 1 appendix table.

Abstract: Late Cretaceous plutonic rocks of 6 gabbroids, and 75 granitoids, all belonging to ilmenite series, were re-examined by polarized XRF method. The gabbroids are relatively abundant in the south of the studied region, implying more in-put of heat and mafic magmas from the upper mantle to the lower crust. The MgO/Fe_2O_3 ratio of the gabbroids reveal regional variation being MgO-rich to the south, which would reflect generation depth of the mafic magmas. The granitoids are classified into I type and S type. The I-type granitoids occur most widely and divided into five zones. Their average silica contents vary from the Median Tectonic Line to the north as follows: Shinshiro-Shitara zone (60.1 % SiO_2), Asuke zone (64.2 %), Toyota-Akechi zone (70.0 %), Sanagesan-Obara zone (73.9 %) and Seto zone (75.2 %). This regional variation was considered to reflect chemical heterogeneity of the infracrustal source rocks, rather than the magmatic differentiation.

Granitoids of the Okazaki-Busetsu zone, represented by garnet-bearing muscovite-biotite granites, occur in the highest metamorphic grade zone, and is felsic (average SiO_2 70.2 %), peraluminous (A/CNK over 1.1), and thus be called S type. Because of the highest heat flow rate in the Okazaki-Busetsu zone, even supracrustal rocks were converted to magmas and formed the S-type granites. Both I and S type granitoids are often heterogeneous in the foliated parts, as compared with massive granitoids of non-metamorphic terrains. The heterogeneity can be considered due to different original compositions of the source materials and/or formed by differential regional stress during the flow movement of the solidifying magmas. Lack of hydrothermal mineralization in the south where metamorphic roof-pendent still remain, can be explained by a deep emplacement level (～15 km) and small degree of fractionation of these granitic magmas.

Keywords: Late Cretaceous, granitoids, meta-basite, ilmenite series, I type, S type, major elements, minor elements

1. Introduction

Late Cretaceous-Paleogene granitoids constituting the largest batholith in the Inner Zone of Southwest Japan (Fig. 1), are divided, from south to north, into barren Ryoke Belt, Cu-Sn-W mineralized Sanyo Belt, and Pb-Zn-Mo mineralized Sanin Belt (Ishihara, 1978). The Ryoke and Sanyo granitoids belong to ilmenite series, whereas the Sanin granitoids are of magnetite series. Each belt is a narrow zone, but the Ryoke granitoids occur most widely in the Mino-Mikawa Mountains of Gifu-Aichi Prefectures, Chubu District. The granitoids are all composed of magnetite-free quartz dioritic, granodioritic and granitic compositions, and intrude into the regional metamorphic rocks of the Ryoke Belt. The granitoids are considered to be generated in continental crust of both igneous and sedimentary source-rocks, which were once homogenized, by the heat brought up with gabbroic magmas from the upper mantle (see Ishihara and Matsuhisa, 2002 for the details).

Chemical compositions of these granitoids were analyzed by "wet"-method during 1960s (e.g., Ishihara *et al.*, 1969; Ishihara 1971), which were re-analyzed by the polarized XRF method later, and found that (1) low correlation coefficients obtained from MnO (0.83), P_2O_5 (0.85), Al_2O_3 (0.87) and Na_2O (0.88), and that (2) diversity from unity is low on P_2O_5 (0.79) and MnO (0.83) but is high on K_2O (1.15). It should be emphasized that the conventionally well known Lawrence Smith's method gave consistently low values on the K_2O contents relative to the XRF values and the agreements were poor on minor components such as MnO and P_2O_5 (Ishihara, 2002).

Previously studied samples from the Ryoke Belt of the Chubu District (e.g., Ishihara and Terashima, 1977)

[1]National Institute of Advanced Industrial Science and Technology (AIST)

[2]School of Earth and Environmental Sciences, University of Wollongong, NSW 2522, Australia

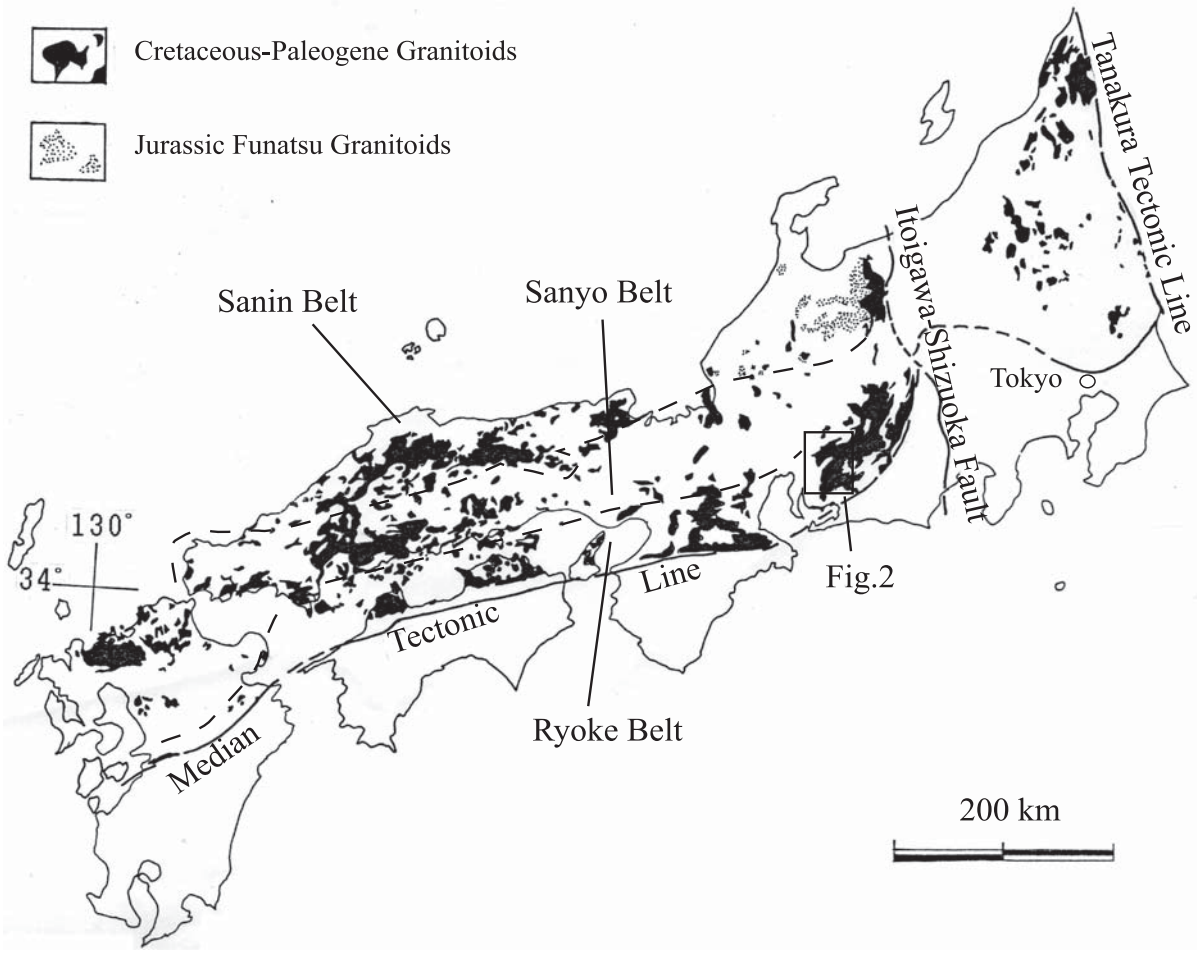

Fig. 1 Distribution of the Cretaceous-Paleogene granitoids in Southwest Japan and locality of the studied area.

also need to be re-analyzed by polarized XRF method. New samples were added and their localities are given in Table 1. All the samples were crushed by jaw and hand crushers made of special steel, then pulverized by agate mortar at the Geological Survey of Japan. Major elements were analyzed on Li-borate pellet by XLAB 2000 polarized XRF machine of Heckel and Ryon (2002), using the Al target (Na, Mg), graphite target (Al, Si, P, S, Fe) and Co target (K, Ca, Ti, Mn). Minor elements were analyzed on the powders by using the graphite target (S, Cl), Co target (V, Cr), Mo target (Co, Ni, Cu, Zn, Ga, Ge, As, Br, Rb, Sr, Hf, Ta, W, Tl, Bi), Pd target (Y, Zr, Nb, Mo, Th, U), and Al_2O_3 target (Cd, In, Sn, Sb, Te, Cs, Ba, La, Ce). The obtained results were corrected by the software of the Spectro Analytical Instrument Ltd. H_2O analysis was done by conventional method. All the analyses were made by Bruce W. Chappell at the Macquarie University. The senior author is responsible for interpretation of the results.

For analysis of rare earth elements, the pulverized sample was digested in near 100 % concentrated 3.0 ml aqua regia, a 3:1 mixture of concentrated hydrochloric (HCl) and concentrated nitric acids (HNO_3) at 90 °C in a microprocessor-controlled digestion box for 2 hours. The solution was then diluted and analyzed by means of inductively coupled plasma mass spectrometry (ICP-MS) using a Perkin Elmer SCIEX ELAN 6,100 at Activation Laboratories Ltd., Ontario, Canada.

All the results are listed in the appendix, and are interpreted in the following paragraphs. These results can also be compared with massive granitoids of the Sanyo Belt, which were analyzed by the same XRF method (Ishihara and Wu, 2001; Ishihara, 2002).

2. Geological Outline

The studied plutonic rocks of the Chubu District are distributed in the Ryoke metamorphic belt between the Median Tectonic Line and the Sanagesan range (Fig. 2). The metamorphic rocks are originally accretionary complex of Jurassic age, composed mostly of fine-grained sandstone and some shale. Chert is also predominant in the southernmost part. General strike of

Table 1 Locality of the newly collected analyzed samples.

Numbers	Locality	Rock type and magnetic susceptibility
1, RG37	Minami-Shitara, Tsukute, Iwanami south 1 km	Fine diorite, SI=0.42-0.63 x 10^{-3}
2, RG38	ditto, Tsukute, Higashi-Takamatsu	Fine quartz diorite, SI=0.21-0.38 x 10^{-3}
3, RG39	ditto, Tsukute, Yasunaga, Kendai	Fine quartz diorite, SI=0.22-0.31 x 10^{-3}
8, RG10	ditto, Tsukute, Hongo	Medium gabbro (cumulate?), SI=0.65-0.70 x 10^{-3}
9, RG06	ditto, Shitara, Mitsuhashi	Fine gabbroic enclave, SI=0.46-0.55 x 10^{-3}
10, RG07	RG07 to RG 09 samples were	Medium granodiorite, SI=0.36-0.42 x 10^{-3}
11, RG08	taken from the same road-cut outcrop	Fine leucogranodiorite, SI=0.20-0.30 x 10^{-3}
12, RG09	at the entrance to Mitsuhashi	Fine biotite aplite, SI=0.08-0.10 x 10^{-3}
13, RG32	ditto, Ure east, 300 m	Very fine gabbro, SI= 0.33-0.36 x 10^{-3}
14, RG31	Kita-Shitara, Shitara,Ure south 2 km, Seiryu Park	Fine garnet diorite, SI=0.25-0.68 x 10^{-3}
15, RG33	ditto, Ure east 300 m	Fine granite, SI=0.02 x 10^{-3}
23, 52002	Okazaki. Taki-machi, Oiri 21-1, Quarry	Medium, two-mica granite(+13.5*), SI=0.06-0.08 x 10^{-3}
24, 52003	The samples 52003 to 6 were taken from	Fine biotite granodiorite(+11.5*), SI=0.09-0.12 x 10^{-3}
25, 52004	the Nakane Sekizai quarry where the	Medium, two-mica granite(+11.8*), SI=0.06-0.08 x 10^{-3}
26, 52005	granite shows compositional banding of	Fine two-mica granite(+13.6*), SI=0.05-0.08 x 10^{-3}
27, 52006	E-W to N70°W strike and steep S dip	Very fine, muscovite granite(+13.5*), SI=0.03-0.05 x 10^{-3}
28, RG26	Toyota, Natsuyake north 1 km, river floor	Fine gabbro, synplutonic dike, SI=0.38-0.55 x 10^{-3}
29, RG28	ditto, Natsuyake north 1 km, river floor	Brecciated granitic dike, N45°E-35°SE
30, RG27	ditto, Natsuyake north 1 km, river floor	Aplitic dike (80 cm wide), N40°W-70°SW
31, RG29	ditto, Kudariyama, Hanabishi Quarry	Fine quartz diorite, SI=0.30-0.38 x 10^{-3}
32, RG30	ditto, ditto, Hanabishi Quarry	Medium, porphyritic granodiorite, SI=0.28 x 10^{-3}
33, RG36	ditto, Hanabishi Quarry, paired dike with RG35	Fine quartz diorite, SI=0.62 x 10^{-3}
34, RG35	ditto, Hanabishi Quarry	Fine granite, SI=0.18-0.25 x 10^{-3}
38, RG22	Higashi-Kamo, Asuke, Kawabata, river floor	Stretched mafic enclave N70°E-80°N, SI=0.32 x 10^{-3}
39, RG23	ditto, Mafic enclave	Stretched mafic enclave, 7 x 45 cm
40, RG24	ditto, Mafic enclave	Stretched mafic enclave, 8 x 50 cm
41, RG25	ditto, Mafic enclave	Stretched mafic enclave, 20 cm x 1.5 m, SI=0.32 x 10^{-3}
44, SJ10	Higashi-Kamo, Asuke, Kawamo	Very coarse granodiorite foliated, SI=0.15-0.33 x 10^{-3}
45, SJ11	ditto, Asuke, Kunitani-Shirakawa	Fine, leucogranodiorite, SI=0.01-0.03 x 10^{-3}
50, SJ08	Toyota city, Yanami-cho, Toyokawa golf course E	Very coarse granodiorite foliated, SI=0.09 x 10^{-3}
51, SJ09	ditto, 3 km northeast of SJ08	ditto, N80°E-40°N, SI=0.11-0.13 x 10^{-3}
54, FJK	Nishi-Kamo, Fujioka, Fujioka-Mikage quarry	Coarse granodiorite, SI=0.12-0.15 x 10^{-3}

(+13.5*), implying whole-rock $\delta^{18}O$ value (‰). SI is magnetic susceptibility measured by Kappameter KT-5.

the rocks is ENE-WSW to E-W. The metamorphic rocks are classified from north to south, 1: biotite zone (slate and mica schist), 2: cordierite zone (mica schist), and 3: sillimanite zone (banded gneiss), distribution of which is shown in Fig. 2. The metamorphic rocks of the Zone 1 do not occur in the studied area.

The plutonic rocks intrude into the metamorphic rocks and the early-formed metabasites (Fig. 3A, B), and give them thermal effect. Radiometric ages of the intrusive rocks, as CHIME-monazite age, Rb-Sr whole-

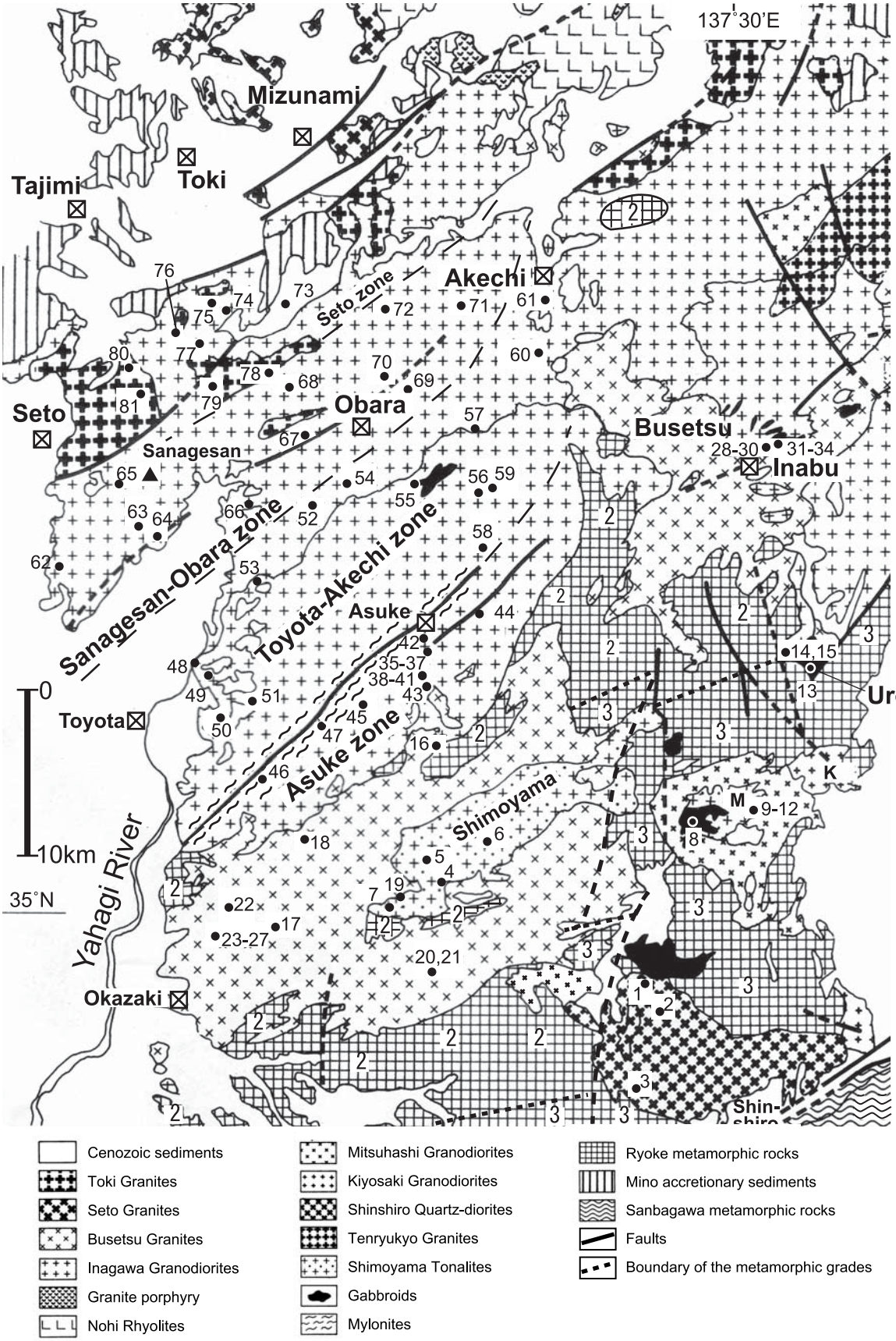

Fig. 2 Geologic map and sample localities of the studied granitoids. Geologic map was taken from Nakai (1990) but partly revised. Bold numerals of 3, sillimanite zone; 2, cordierite zone. From Makimoto *et al.* (2004). M, Mitsuhashi, K, Kiyosaki

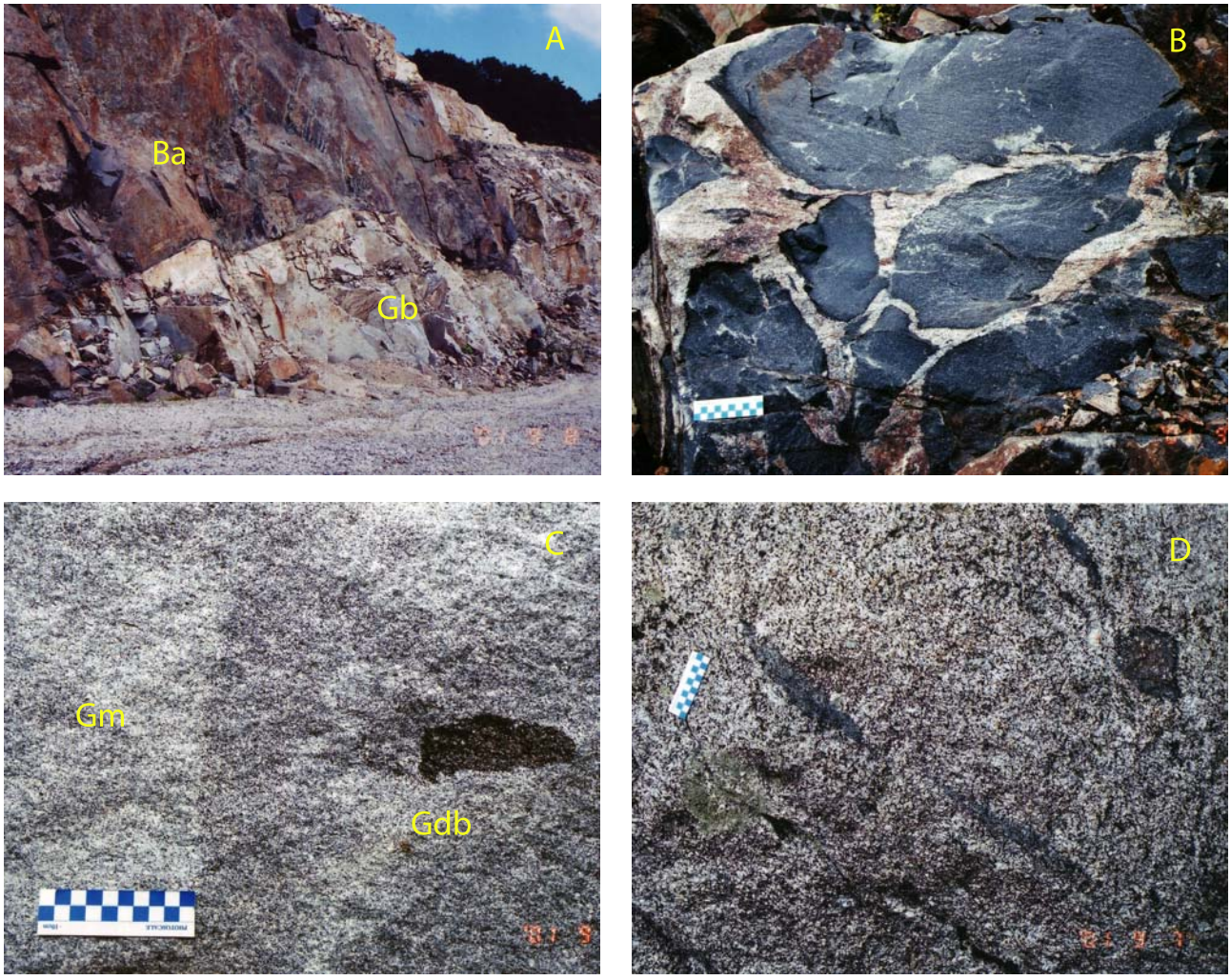

Fig.3 A:Outcrop of metabasite (Ba) intruded by leucogranite of the Busetsu Granite (Gb), Hanabishi quarry, Kudariyama, Natsuyake-cho, Toyota city. B:Metabasite mingled with the leucogranite, Hanabishi quarry. C:Heterogeneous Busetsu Granite with biotite-rich enclave. Gdb, biotite granodiorite; Gm, muscovite-biotite granite. Nakane-Sekizai quarry, Okazaki city. D:Two generations of mafic enclaves: one strongly foliated; the other with weak elongation. Kawabata, south of Asuke township.

rock isochron and whole-rock-mineral isochron age, and K-Ar mineral age, range from 95 to 75 Ma (see, summary of Makimoto *et al.*, 2004). Nakai and Suzuki (2003) summarized the CHIME monazite ages and the cross-cutting relationships of the Ryoke granitoids as shown in Fig. 4.

In the figure, the plutonic rocks are classified into the pre-Nohi and post-Nohi Rhyolites, which have been considered volcanic equivalent of the granitoids, but these Rhyolites occur only in the northernmost part of the Ryoke Belt, and the cross-cutting relationships to most of the Ryoke granitoids in the south are not observed directly but one with the Inagawa granodiorite at the northwestern part. With this limitation and the fact that granitoids are often affected by the crustal components, the granitoids here are described regionally from south to north, in following high to low grades of the Ryoke metamorphic rocks.

2.1 Plutonic rocks in the south

At just north of the Median Tectonic Line, intruded into the sillimanite metamorphic zone discordantly is the Shinshiro biotite-hornblende-quartz diorite containing abundant mafic enclaves with weak foliation. Fine-grained mafic intrusives and granodiorites occur associated with this pluton around the northewestern rim (Fig. 2). No ore deposits are found in the southern zone, although the intruded rocks are remaining abundantly.

To the north, a composite pluton with 8 km E-W and 9 km N-S occurs also in the sillimanite metamorphic zone, which is the classic site where Koide (1958) proposed Mitsuhashi and Kiyosaki Granodiorites, which are followed by Kutsukake (1997a, 2001). These granitoids

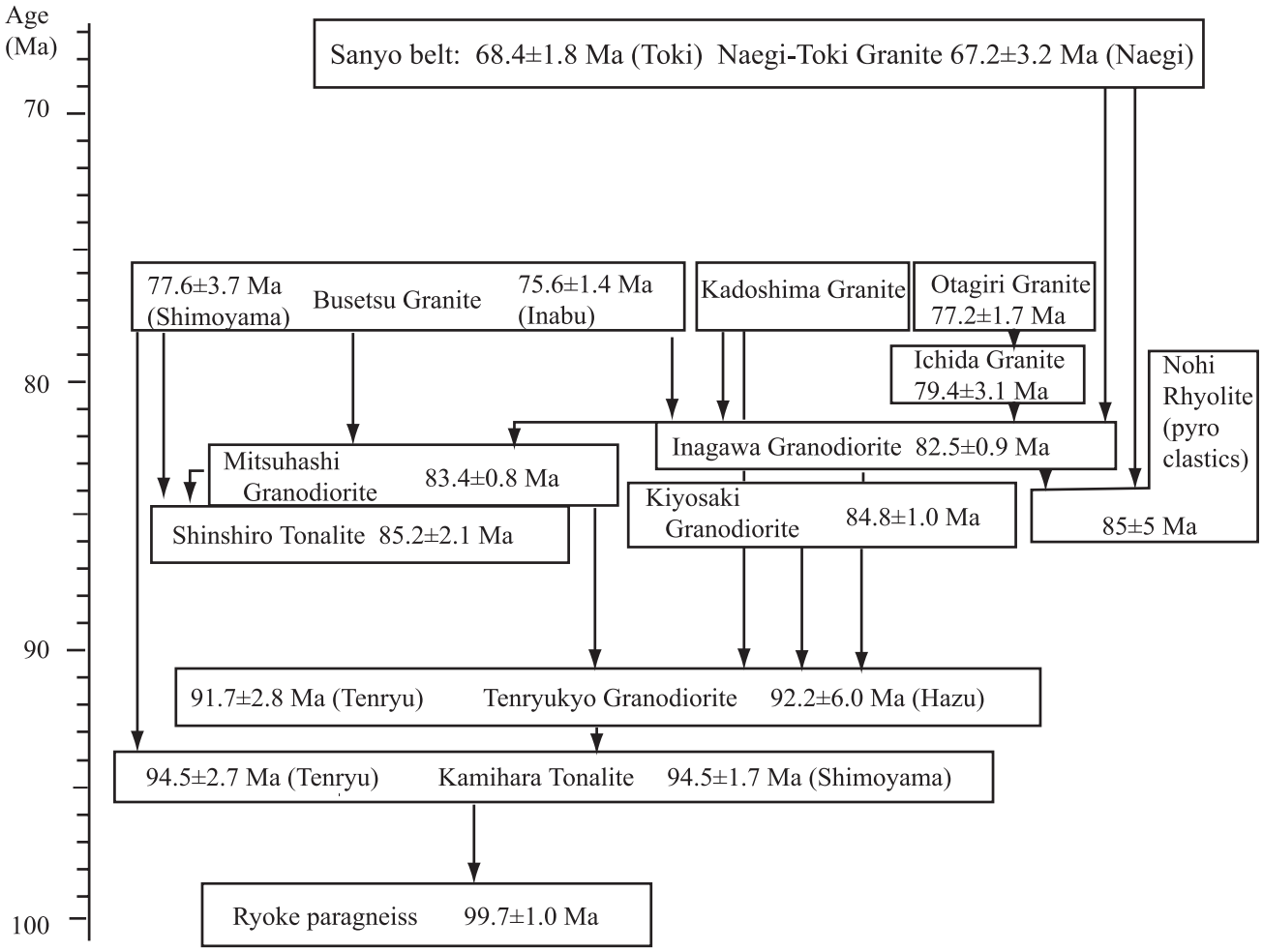

Fig. 4 Summary of intrusive relationships among the Ryoke granitoids and the Nohi ignimbrites (from Nakai and Suzuki, 2003).

seem to constitute one single pluton intruding into the Ryoke metamorphic rocks, and thus is called Mitsuhashi pluton in this paper. This pluton is essentially biotite-hornblende granodiorite, but contains more mafic phase and mafic enclaves, or more felsic phase than the granodiorite locally. Garnet which coexists rarely with hornblende in general, can be observed in this I-type granodiorite, as well as allanite (Kutsukake, 1993) occurring in the granodiorite. The garnet was considered to be formed by the wall-rock assimilation under low oxygen fugacity and high Fe/Mg ratios of the Mitsuhashi magmas (Kutsukake, 1997a, c). Foliation is only limited to the marginal phase.

To the west of this pluton, Shimoyama Quartz Diorite occurs mostly in the sillimanite and cordierite zones (Fig. 2). This is strongly foliated K-feldspar-free quartz diorite showing a basin structure (Nakai, 1990), but the mafic silicates are generally biotite and hornblende. This body occupies a central part of large Busetsu Granite pluton; their intrusive sequence is that felsic Busetsu Granite is always later than the Shimoyama Quartz Diorite (Nakai *et al.*, 1985).

In this zone of the Shinshiro, Shimoyama, Mitsuhashi and Ure intrusive bodies, which is called as the Shinshiro-Shitara zone, an average of the studied plutonic rocks has 60.1 % SiO_2 and A/CNK=0.9, i.e., the least silicic, and most mafic and calcic among the studied six zones (Table 2).

The zone to the north is the famous stone industry area of Okazaki City. Fine- to medium-grained muscovite-biotite granite, which has been called Busetsu Granite, is major source for the traditional stone industry. Although some mafic rocks occur in the northeasternmost part, this zone is characterized by high SiO_2 (an average of 70.3 %) and A/CNK ratio (1.06, peraluminous, Table 2.).

This pluton, striking northeasterly for more than 70 km with the width of 7 to 13 km, is the most felsic phase in the southern Ryoke Belt. No mafic enclaves but small sedimentary ones are commonly observed (Fig. 3C). In the northeastern part at Natsuyake, just NE of Inabe (Fig. 2), metabasites are intruded by leucogranite (Fig. 3A, B), which may not be a proper member of the Busetsu Granite. The Busetsu Granite

Table 2 Average major compositions of the studied granitoids in each zone and the Naegi Granite.

Zone	I	II	III	IV	V	VI	Naegi
SiO_2wt.%	60.11	70.32	64.16	69.98	73.01	75.15	76.79
TiO_2	0.83	0.42	0.79	0.31	0.22	0.14	0.04
Al_2O_3	16.09	14.65	15.28	15.14	13.60	12.84	12.75
Fe_2O_3	7.07	3.33	5.92	2.86	2.31	1.60	1.07
MnO	0.12	0.07	0.10	0.05	0.05	0.06	0.02
MgO	3.16	0.71	1.55	0.65	0.53	0.30	0.04
CaO	6.03	2.76	5.00	3.66	2.10	1.30	0.65
Na_2O	3.22	3.16	3.18	3.22	3.03	3.22	3.57
K_2O	2.18	3.62	3.05	3.31	4.48	4.64	4.82
P_2O_5	0.19	0.15	0.16	0.07	0.06	0.03	<0.01
Sum	99.00	99.19	99.19	99.25	99.40	99.28	99.75
A/CNK	0.90	1.06	0.88	0.99	1.00	1.01	1.04
Rb/Sr	0.22	0.66	0.37	0.41	1.43	3.07	25.60

I. Shinshiro, Shimoyama and Mitsuhashi pluton (n=12); II. Okazaki-Busetsu zone (n=19); III. Asuke zone (n=13); IV. Toyota -Akechi zone(n=14) ; V. Sanagesan - Obara zone (n=11); VI. Seto zone (n=9). The Naegi Granite (n=5), an average of the west body from Ishihara (2002)

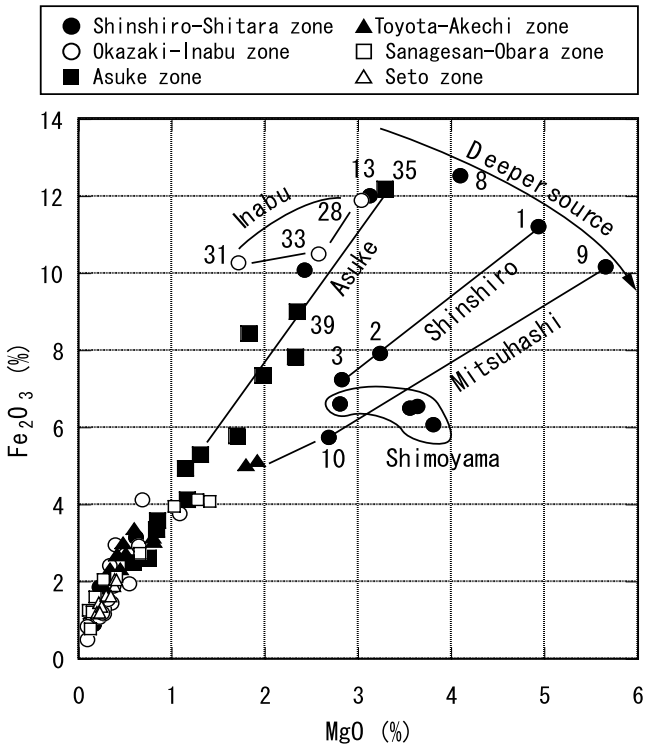

Fig. 5 Total iron vs. MgO diagram of the studied plutonic rocks.

has generally muscovite-biotite assemblage but biotite granodiorite also occur (Fig. 3C). Garnet is common in muscovite-dominant phase; monazite is predominant all over the rocks, thus the phosphorous content is high, as compared with biotite granites in other regions. Small muscovite pegmatites are commonly distributed in and around the muscovite-biotite granite.

2.2 Plutonic rocks in the north

Plutonic rocks in the north and northwest are exposed most widely and the roof metamorphic rocks are hardly seen. They are composed of hornblende-biotite and/or biotite assemblage and meta-aluminous, i.e., I type. They are very coarse-grained to medium-grained, and are granodiorite to granitic in composition. The granodiorites, which are often called Inagawa (or Sumikawa) Granite, may contain small mafic bodies and mafic enclaves, often foliated. The foliation is locally strong (Fig. 3D), particularly along NE-faulting in the Asuke zone (Fig. 2).

To the north, the plutonic rocks become felsic. The Akechi zone consists of the average SiO_2 content of 64.2 %, but the next zone of the Toyota-Akechi zone has 70.0 % (Table 2). Biotite granite increases in amount to the further north, and the average SiO_2 contents are 73.0 % for the Sanagesan-Obara zone, and 75.2 % for the Seto zone. Aplitic granites occur in the high mountain range along the Sanagesan to the northeast (i.e., Mikuniyama).

3. Magnesium vs. total iron ratios of mafic intrusive rocks

Mafic plutonic rocks of the Ryoke Belt are composed of coarse-grained gabbroic cumulate (Kutsukake, 2000;

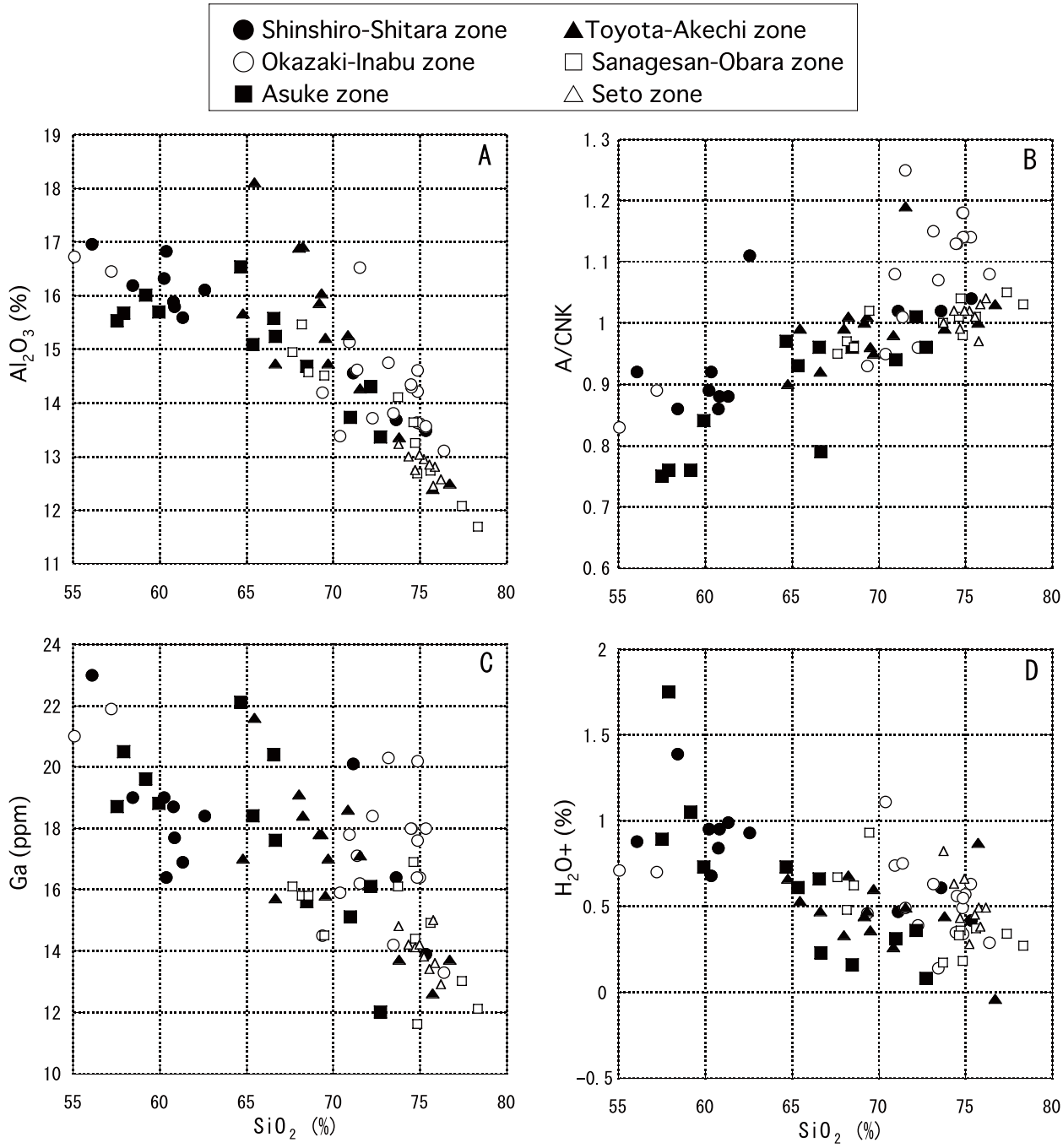

Fig. 6 Silica vs. Al_2O_3, A/CNK. Ga and H_2O+ of the Ryoke granitoids.

Nakajima *et al.* 2004) and fine-grained diabasic rocks known as "meta-basite" (Kutsukake, 1975). The diabasic rocks are earlier than the granitoids (Fig. 3A), or are simultaneous with the granitoids (Fig. 3B). Thus, the mafic magmas are intimately related to the granitic magmatism in the studied area. Moreover, these rocks tend to occur sporadically but in the highest metamorphic grade, sillimanite zone (Fig. 2), implying that the metamorphic heat may have brought up with the mafic magmas from the upper mantle. Kutsukake (1975) identified either high-Al tholeiite or calc-alkaline dolerite in the mafic rocks; yet further detailed studies are still necessary.

In the MgO vs. total iron as Fe_2O_3 diagram, the studied mafic rocks are classified into two by their MgO/Fe_2O_3 ratio (Fig. 5). The high MgO/Fe_2O_3 group includes the metabasite occurring in and near the Shinshiro and Mitsuhashi plutons. One low MgO/Fe_2O_3 rock (0.33, No. 8 of the Mitsuhashi pluton) is considered as cumulate (Nakajima *et al.*, 2004); thus

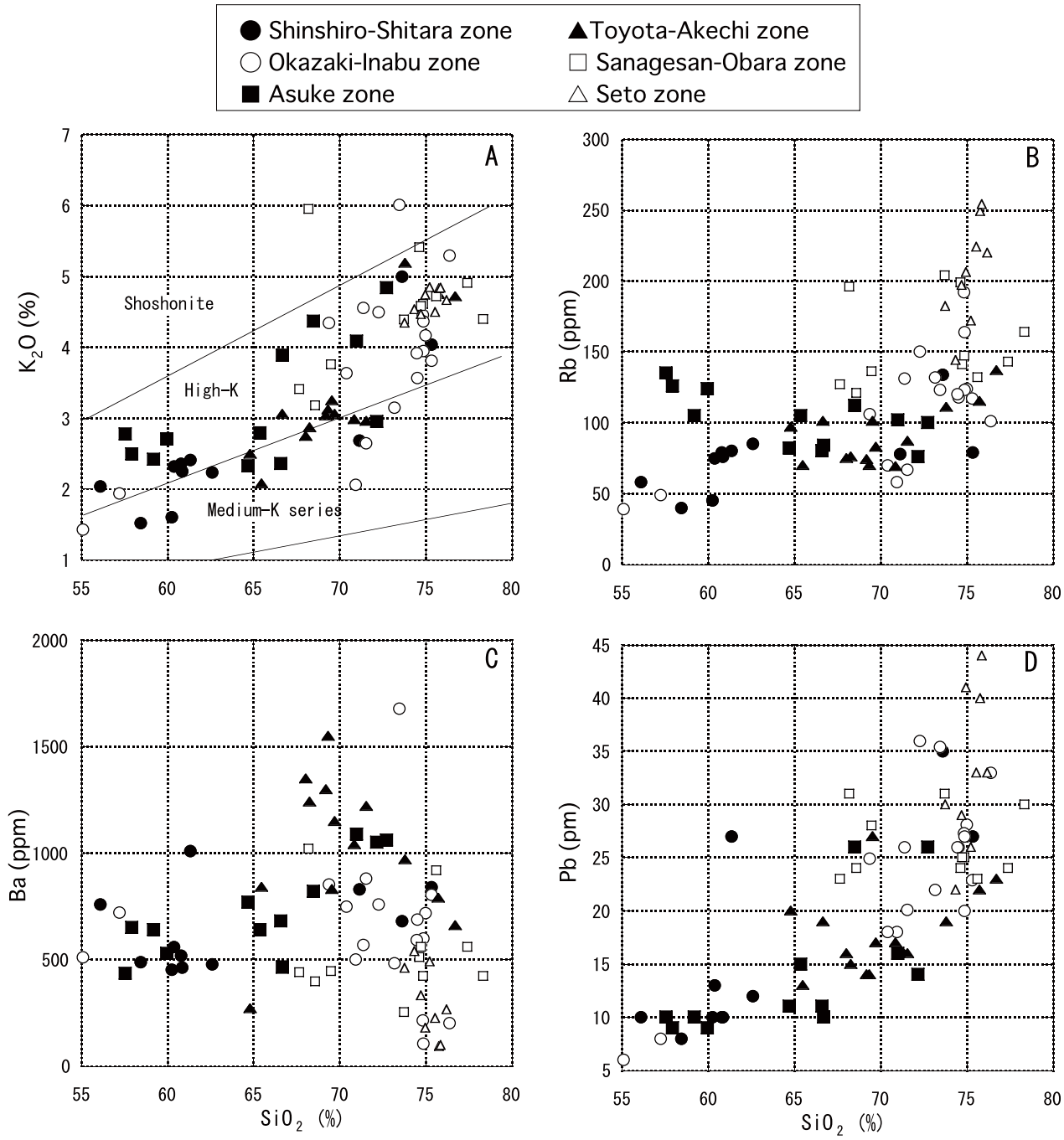

Fig. 7 Silica vs. K_2O, Rb, Ba and Pb of the Ryoke granitoids.

different from the main trend of the Mitsuhashi pluton. The Shimoyama Quartz Diorite belongs also to this group. On the other hand, the low MgO/Fe_2O_3 group are those occurring in the Asuke zone and Inabu area, which are located to the north of the high MgO/Fe_2O_3 group.

MgO/Fe_2O_3 of gabbro and quartz diorite of the Shinshiro pluton vary from 0.44 to 0.39, and the average is 0.42. The mafic phases of the Mitsuhashi pluton vary from 0.47 to 0.56, and the average is 0.52. Quartz diorite of the Shimoyama body has the highest MgO/Fe_2O_3 of 0.62 - 0.42 (average 0.54) at 61 SiO_2% (see Appendix, Nos. 4 - 7). Therefore the Shimoyama Quartz Diorite is most magnesian, then the Mitsuhashi and the Shinshiro Granodiorites (Fig. 5).

On the contrary, mafic enclave to the south of Asuke township in the Asuke zone (Fig. 2) has MgO/Fe_2O_3 ratio of 0.27 (No.35, Appendix). The other plutonic rocks, stretched mafic enclave at south of Asuke township (No. 35, Fig. 5), and mafic dikes at Ure and Inabu-

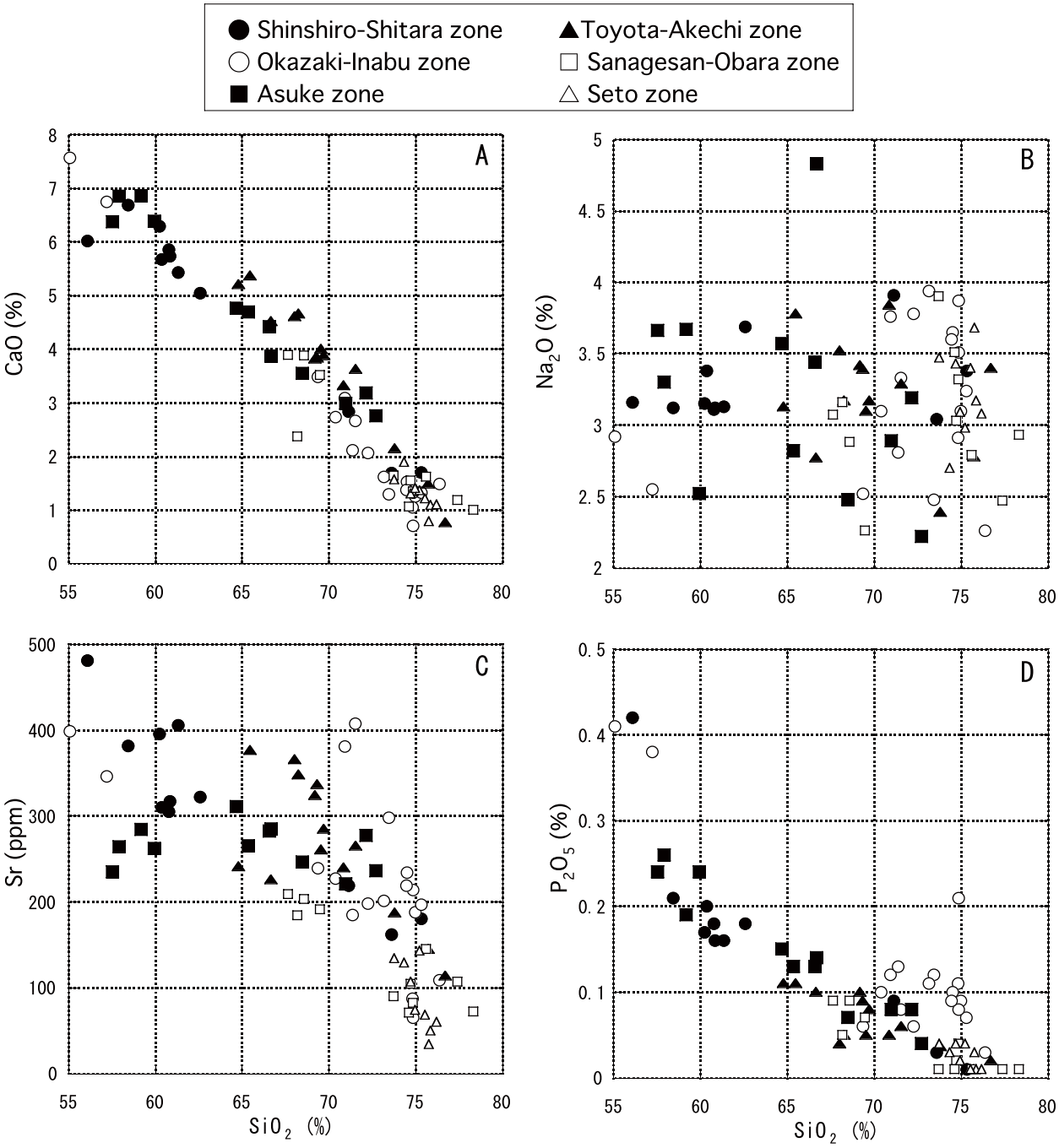

Fig. 8 Silica vs. CaO, Na_2O, Sr and P_2O_5 of the Ryoke granitoids.

Natsuyake (Nos. 13, 28, 31, 33, Fig. 5) are most dominant in iron. Therefore, a clear zoning is seen in the mafic plutonic rocks in the north-south direction. This regional variation is considered reflecting difference of the source rocks due to different depth of the magma generation. These mafic magmas have been mixed with granitic magmas generated within the continental crust.

4. Variation diagrams for the granitoids

Chemical components and zircon saturation temperature (Watson and Harrison, 1983) are plotted against silica contents (Figs. 6 - 12). The examined rocks are classified in the zone units, namely from south to north, Shinshiro-Shitara zone including the Shinshiro, Shimoyama, Mitsuhashi and Ure bodies, Okazaki-Inabu zone, Asuke zone, Toyota-Akechi zone, Sanagesan-Obara zone, and Seto zone, the local names of which

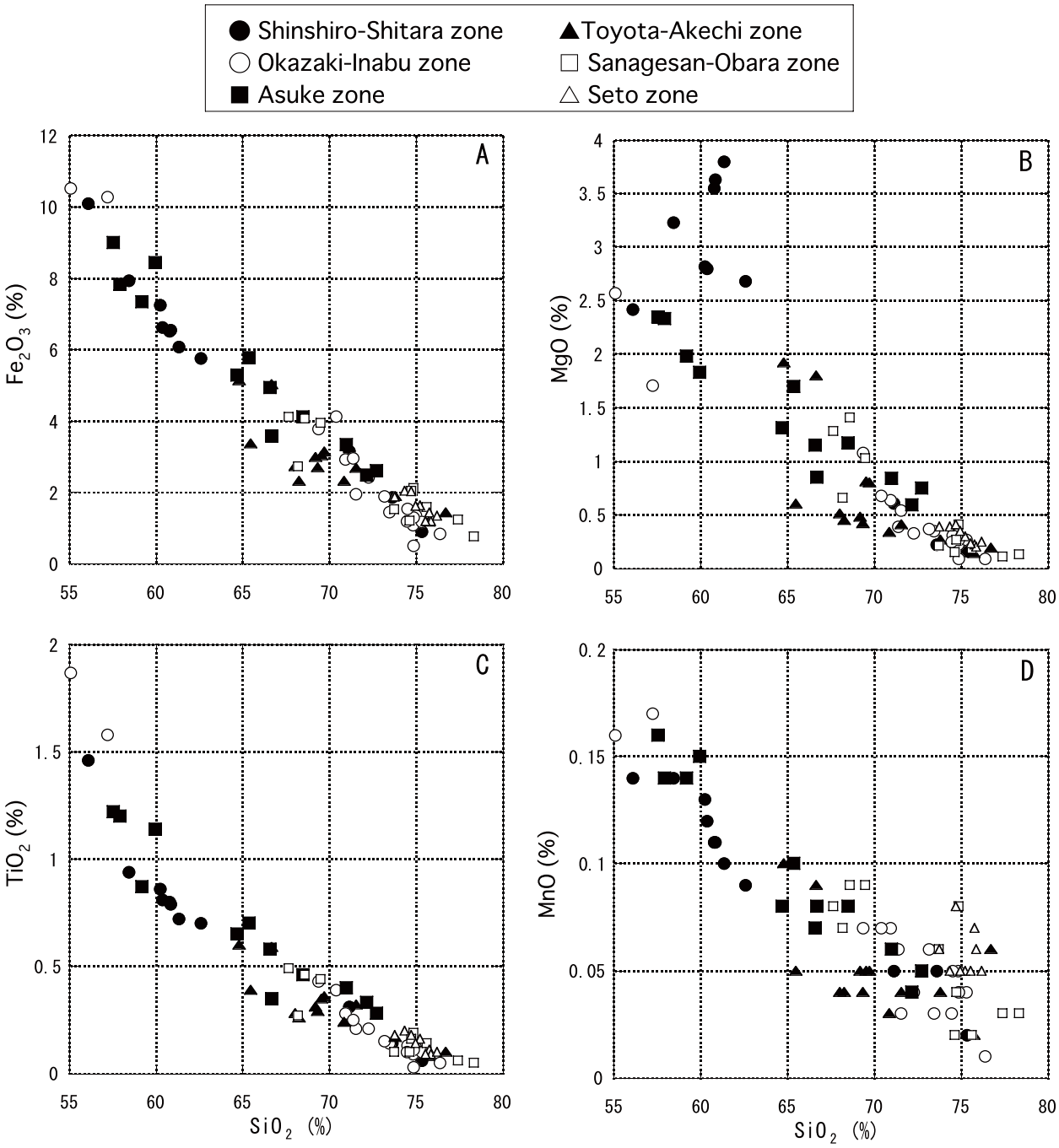

Fig. 9 Silica vs. Fe_2O_3, MgO, TiO_2 and MnO of the Ryoke granitoids.

are shown in Fig. 2. As mentioned previously, the studied plutonic rocks are free of magnetite and have hornblende-biotite and/or biotite assemblages, except for the Busetsu Granites of the Okazaki-Inabu zone, which has (garnet-)muscovite-biotite or biotite assemblage. The granitoids are non-adakitic (Sr/Y<22, Ishihara *et al*., 2005), but a few high Sr/Y values are observed in the Shinshiro-Shitara zone (e.g., Nos. 4 and 12), and the Okazaki-Busetsu zone (Nos. 16 and 19).

4.1 Major elements

Al_2O_3 contents are high in the granodiorite (SiO_2 65 - 71 %) of the Toyota-Akechi zone and many of granites (SiO_2 75 - 77 %) of the Okazaki-Inabu zone (Fig. 6A), but the alumina saturation index (A/CNK) is high mostly in those of the Okazaki-Inabu zone, which are mostly garnet-bearing muscovite-biotite granite. In the main body of the Okazaki area (Nos. 16-27, Appendix), the value ranges from 0.93 to 1.25 and the average is 1.13, which exceeds 1.1 for the S-type granite

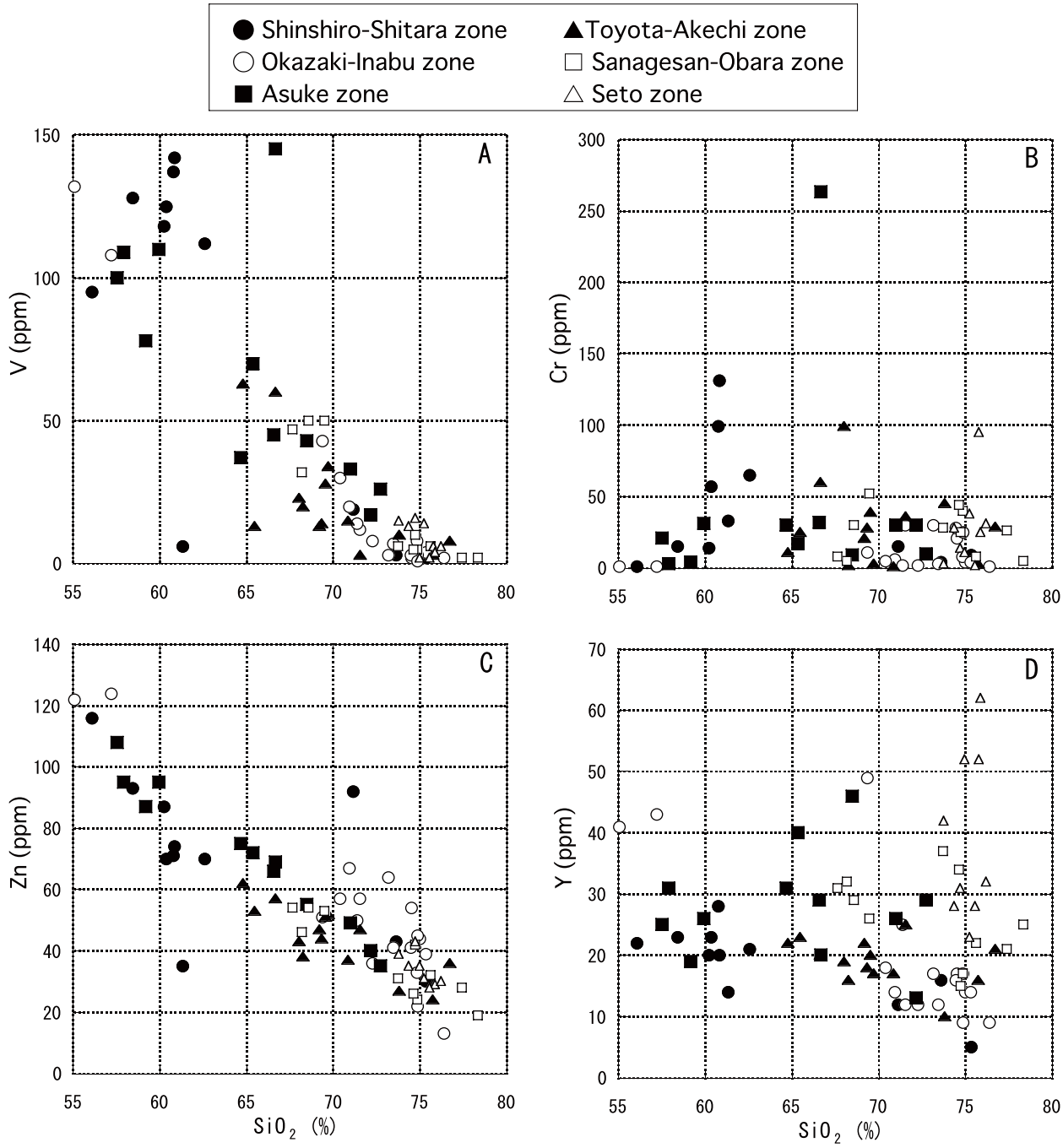

Fig. 10 Silica vs. V, Cr, Zn and Y of the Ryoke granitoids.

(Chappell and White, 1974). Some garnets are observed in the granodiorite with hornblende-biotite assemblage in the Mitsuhashi pluton, whose A/CNK is 1.11 (No. 10, Appendix). All the other quartz diorite and granodiorite have the A/CNK lower than 0.92.

Ga, which tends to substitute Al in feldspars, is fairly high as calc-alkaline series. Ten samples contain more than 20 ppm Ga (Fig. 6C), which are similar range of A-type Mumbulla and Gabo batholiths (Ishihara and Wu, 2001). $H_2O(+)$, which may represent amounts of such hydrous minerals, as hornblende, biotite and muscovite, decreases with increasing silica contents.

On the K_2O-SiO_2 diagram, most of the studied granitoids are plotted from the medium-K to high-K series field (Fig. 7A). Two extremely high values are muscovite-rich band in the Busetsu Granite (No. 22, Appendix) and K-feldspar-rich part of the Inagawa Granodiorite in the Sanagesan-Obara zone (No. 62, Appendix). Low K_2O rocks are predominant in granitoids of the Shinshiro-Shitara zone, where the

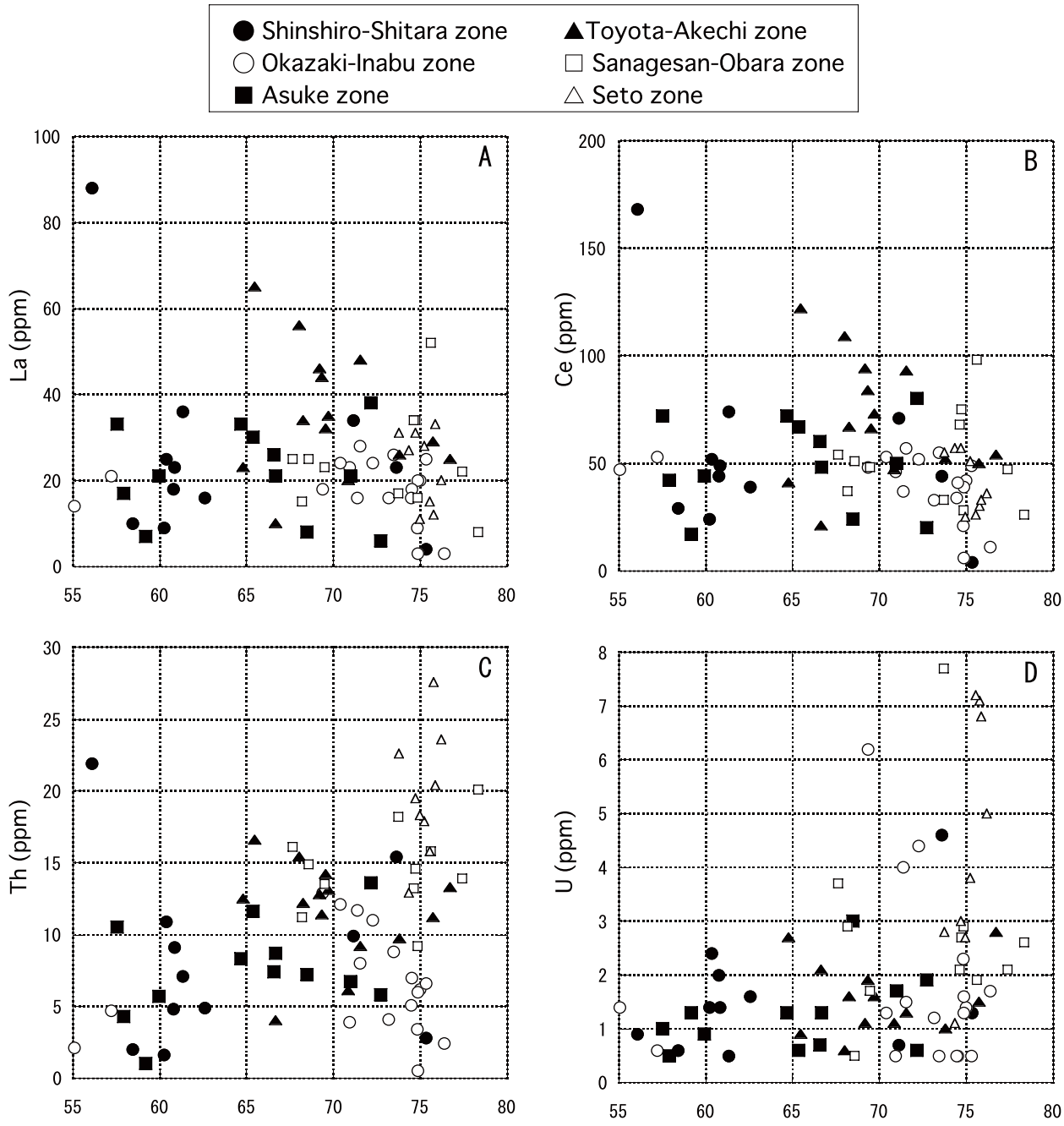

Fig. 11 Silica vs. La, Ce, Th, and U of the Ryoke granitoids.

granitoids are the most mafic, and in some of the Asuke and Toyota-Akechi zones.

Rb follows generally K content, which is also shown in the Fig. 7B diagram. Rb-rich rocks (more than 100 ppm) of the mafic granitoids (SiO_2 57 - 60 %) from the Asuke zone are elongated mafic enclaves in the host granodiorites. The other Rb-rich rocks are the granites of the Seto zone. Rb contents of the Busetsu Granite are low for their K_2O contents (Fig. 7B). Ba contents are correlated positively with many of the studied rocks (Fig. 7C). However, the contents are low in granodiorites and granites of the Sanagesan-Obara and Seto zones from the north. The Busetsu muscovite-biotite granites are also low for the high K_2O contents. Pb, on the other hand, is positively correlated with K_2O, implying its substitution of K in K-feldspars.

CaO contents are negatively correlated well with the silica contents, while no correlation is seen on the Na_2O contents (Fig. 8A, B). Sr contents are well correlated with CaO contents, except for the mafic enclaves of

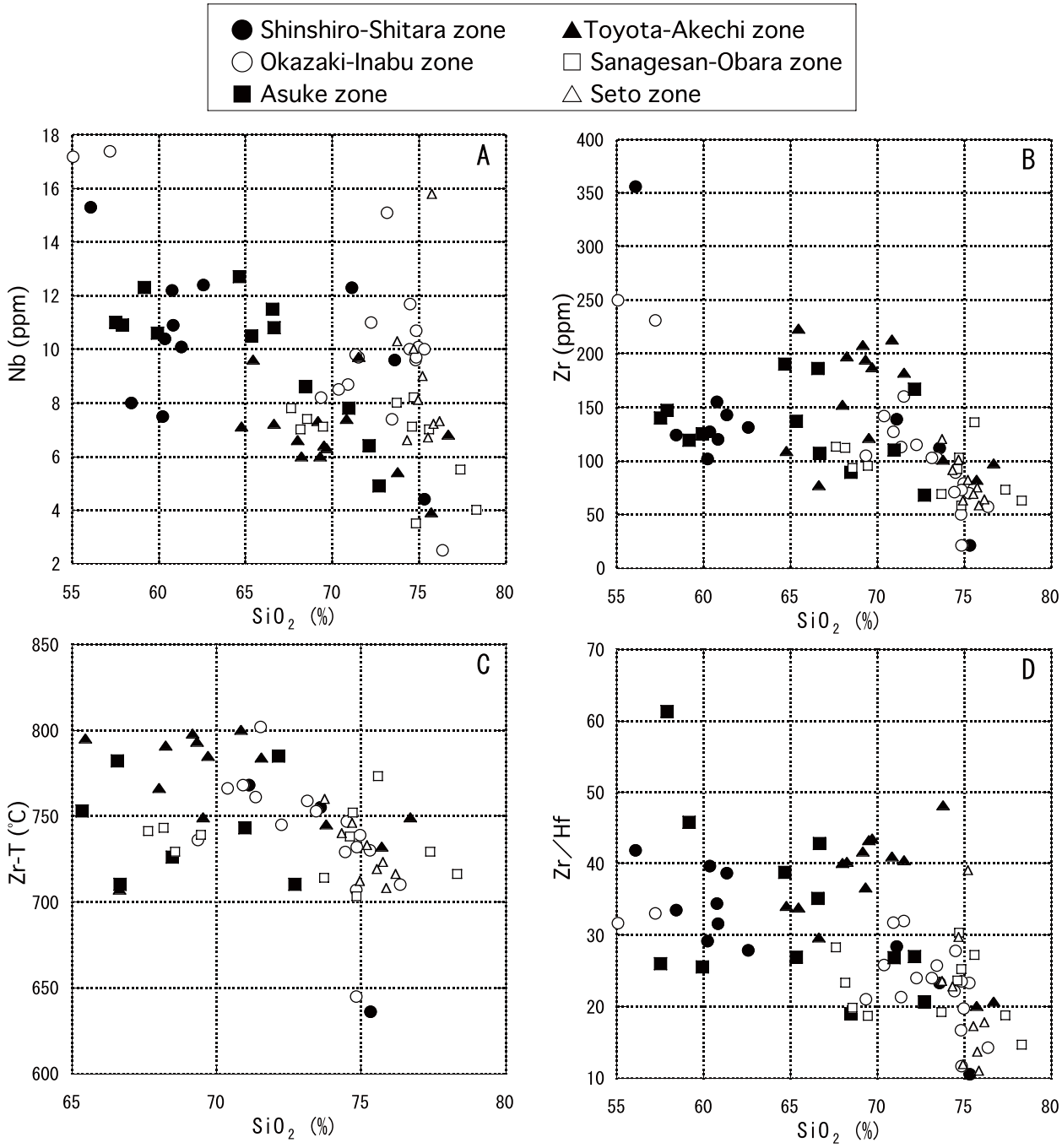

Fig. 12 Silica vs. Nb, Zr, Zr saturation temperature and Zr/Hf of the Ryoke granitoids.

the Asuke zone, which are low in Sr (<300 ppm), but high in CaO. Many of the muscovite-biotite granites of the Okazaki-Inabu zone are enriched in Sr (Fig. 8C). P_2O_5 contents are generally correlated with CaO contents. Many of the muscovite-biotite granites of the Busetsu pluton are rich in P_2O_5 (Fig. 8D), having high P/Ca ratio. The high contents mostly due to abundant occurrence of monazite in the muscovite-biotite granites.

The total iron as Fe_2O_3 is negatively correlated with silica contents throughout all the bodies (Fig. 9A). MgO contents (Fig. 9B), on the other hand, are rich in the mafic granitoids of the Shinshiro-Shitara zone, i.e., southern part. These granitoids are relatively low in both the TiO_2 (Fig. 9C) and MnO contents (Fig. 9D). MnO contents are relatively enriched in the granitoids of the Sanagesan-Obara and Seto zones, i.e., northern part.

4.2 Minor elements

Vanadium may be contained in mafic silicates, because no magnetite is present in the studied rocks. V

contents are positively correlated with the Fe_2O_3 contents. The contents are relatively high in the mafic granitoids of the Shinshiro-Shitara zone in the south (Fig. 10A). No correlation is observed in the Cr vs. silica diagram (Fig. 10B). Zn is negatively correlated with the silica (Fig. 10C), implying that zinc is substituting ferrous iron in the mafic silicates. Y contents are uniquely distributed. The high values are seen in the biotite granites of the Seto zone. This element is also high in the granodiorite and granite of the Sanagesan-Obara zone, and granodiorites of the Asuke zone.

Both La and Ce contents are erratic, like those of Y, and are not correlated with the silica contents (Fig. 11A, B). These elements are somewhat rich in some granitoids of the Toyota-Akechi zone. U and Th contents are generally high in the high silica rocks, especially on those of the Seto and Sanagesan-Obara zones (Figs. 11 C, D).

Nb contents are negatively correlated with the silica contents (Fig. 12A). The contents are relatively high in the muscovite-biotite granites of the Okazaki-Inabu zone, but are low in the granodiorites of the Toyota-Akechi zone. Nb/Ta ratio varies from 1.1 to 9.7. Zr, which may be solely contained in zircon, is negatively correlated with the silica contents (Fig. 12B). Hf substitutes Zr in zircon because of similar ionic radius of Hf^{4+} (0.79A) and Zr^{4+} (0.80A). Experimentally Zr/Hf ratio of zircon is known to decrease with increasing of magmatic fractionation (Linnen and Keplller, 2002). In the actual measurement, the Zr/Hf ratios vary greatly from 48 to 11, which decrease generally with the increasing of SiO_2 contents. The Zr saturation temperature (Watson and Harrison, 1983) is plotted in the range between 800 and 700 °C for the silica contents of 65 - 77 % (Fig. 12C).

Average compositions of 75 granitoids (>55 % SiO_2) are calculated by the least-square method. The average values of each component intersecting the 55 %, 60 %, 65 %, 70 % and 75 % SiO_2 are given in Table 3. The values of 75 % SiO_2 can be compared with an average of the Naegi granites of the Sanyo Belt, which is an example of highly fractionated, Sn-W mineralized granite (Table 3).

Table 3 Average compositions of the Ryoke granitoids at different SiO_2 percentage. The average values calculated based on the least square method are allocated to the SiO_2 contents. Average composition of the Naegi Granite (Ishihara, 2002; Ishihara and Murakami, 2006) is added for comparison (n=4 or 5).

	Ryoke granitoids					Naegi Granite
SiO_2wt.%	55.00	60.00	65.00	70.00	75.00	76.79
TiO_2	1.31	1.00	0.69	0.39	0.08	0.04
Al_2O_3	17.32	16.38	15.43	14.48	13.53	12.75
Fe_2O_3	9.42	7.39	5.37	3.34	1.31	1.07
MnO	0.15	0.12	0.09	0.07	0.04	0.02
MgO	2.97	2.28	1.59	0.90	0.20	0.04
CaO	7.70	6.17	4.63	3.10	1.56	0.65
Na_2O	3.18	3.19	3.19	3.19	3.19	3.57
K_2O	1.48	2.21	2.94	3.67	4.40	4.82
P_2O_5	0.29	0.23	0.16	0.10	0.03	<0.01
H_2O^+	0.98	0.84	0.70	0.55	0.41	0.52
Sum	99.89	99.90	99.91	99.92	99.93	100.27
Rb ppm	48	72	96	120	144	362
Sr	404	343	281	219	158	12
Ba	683	675	667	660	652	34
Zr	203	175	146	118	89	86
Hf	5.3	5.0	4.6	4.2	3.9	3.7
Nb	12.8	11.4	10.1	8.8	7.5	14.0
Y	28.8	27.2	25.7	24.1	22.5	91.6
La	28.6	27.2	25.8	24.3	22.9	19.1
Ce	64.8	60.0	55.3	50.5	45.7	45.0
V	125.6	95.1	64.6	34.1	3.6	1.7
Cr	34.9	32.2	29.4	26.7	23.9	8.5
Zn	104.9	87.0	69.1	51.2	33.2	22.2
Pb	5.9	11.2	16.5	21.8	27.1	29.5
Ga	21.1	19.6	18.1	16.6	15.1	19.6
Mo	1.6	1.4	1.1	0.8	0.6	<0.3
Sn	0.7	1.1	1.6	2.0	2.5	3.8
Th	5.9	7.5	9.1	10.8	12.4	30.7
U	0.7	1.2	1.6	2.1	2.6	10.4
A/CNK	0.82	0.88	0.94	0.99	1.05	1.04
NK/A	0.37	0.46	0.56	0.65	0.74	0.87
Ga*10000/A	2.31	2.26	2.21	2.16	2.12	2.92
Rb/Sr	-0.4	0.1	0.5	1.0	1.4	29.9
Zr/Hf	40.8	36.5	32.1	27.8	23.4	18.6
Sr/Y	15.3	14.0	12.7	11.4	10.0	0.13
Zr-T(˚C)	757	752	747	742	737	739

5. Heterogeneity in the Ryoke Granitoids

The Ryoke granitoids are heterogeneous in many places, which are found generally in the foliated granitoids. The heterogeneity is best seen in tonalite-granodiorite because of color difference of mafic vs. felsic silicates. Mafic enclaves with irregular boundaries (i.e., magma mingling, Fig. 3B) are fairly common, which are stretched along the foliation in the foliated tonalite-granodiorite. Some examples at the south of Asuke township are given in Fig.3D.

The heterogeneity is also seen in a massive granite of the Busetsu Granite in the Okazaki city area, which has been used in daily life for more than 500 years, and still used for graveyard, statues, mortar (Usuishi), Shinto-shrine gate (Torii), fencing and building. Because the mafic silicates are not hornblende-biotite but muscovite-biotite, the heterogeneity is not as distinct as the hornblende-biotite assemblage rock, thus may

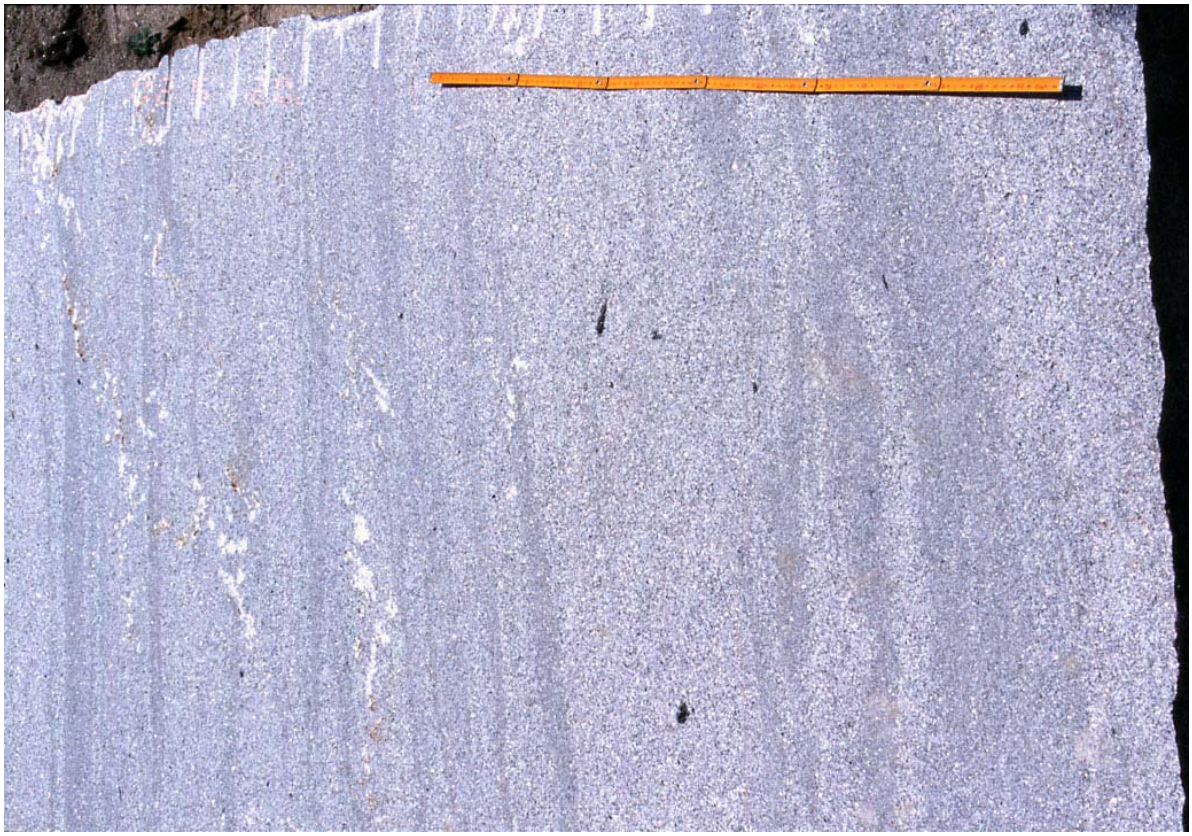

Fig. 13 Muscovite-biotite granite showing heterogenous mineral compositions, Nakane-Sekizai quarry, Aichi Pref. The yellow scale is 1 meter. The black patches are restitic biotite aggregates, which are dominant in salic layers.

be used for the stone industry.

At the Nakane-Sekizai quarry (Nos. 23 - 27, Fig. 2), the granite shows often heterogeneity (Fig. 13), which is shown as faint color difference of black and white, due to the modal change between plagioclase and K-feldspar, and also between biotite and muscovite. However, there are no sharp boundaries among the layers, implying that they are not intrusive relationship. Pegmatitic dikelets are also common cutting through the host granites, some of which contain molybdenite with the Re-Os age of 76.4 +/-0.3 Ma (Ishihara *et al.*, 2002).

Biotite is rich in the dark gray layers but less in the white parts where biotite-rich restite fragments are distinct (see the middle of Fig. 13). Chemical compositions of the representative three phases are shown in the appendix. The biotite-rich parts of muscovite<biotite granites have the femic index (Fe_2O_3+MgO+MnO) of 2.33 % and 1.91 % (Nos. 24, 25, Appendix), muscovite-biotite granite of 1.61 % and 1.48 % (Nos. 23, 26), and muscovite granite of 0.64 % (No. 27).

The whole rock $\delta^{18}O$ data of the three groups are divided into two clear values (Table 1); one with 11.5 to 11.8 permil for the muscovite<biotite granite, while the others with 13.5 to 13.6 permil for the muscovite >biotite granites. Thus, the latter group can be considered to contain much sedimentary components than the former. The regional heterogeneity observed in the Busetsu Granite, therefore, is caused essentially by different source rocks for the granites.

Rb/Sr ratios, which may represent a degree of magmatic fractionation, on the other hand, are constantly low, as 0.5 to 0.7 for the most of rocks (Appendix). Muscovite-rich granite of No.27 at the Nakane quarry is weakly high as 2.5. This granite has lower contents of the REE than the main muscovite-biotite granite (Table 4), and shows slightly enrichment of HREE relative to the main phase granite (Fig. 14). Therefore, this rock may have been fractionated in a small degree but main cause of the heterogeneity is considered to have been formed by differential flow movement of the crystal mush during an early stage of the emplacement.

Kagashima (1999) studied biotite-rich layering, which can be called "schlieren", within porphyritic biotite granite of the Iwafune pluton in non-metamorphic belt. Here, the layering is shown by different proportions of biotite and plagioclase, and the biotite-rich horizon is very high in Rb content, up to 617 ppm, and the Rb/Sr ratios of the five studied layers vary from 46.1 to 4.8. Kagashima (1999) considered the

Table 4 Contents of REE and some trace elements of the Busetsu Granite, as compared with the average Naegi Granite.

	Busetsu Granite			Naegi Granite	
Sample No.	52003	52004	52006	Gb (n=5)	Ga(n=3)
SiO_2 wt.%	73.2	74.5	74.8	76.8	76.5
$\delta^{18}O$ (%)	11.5	11.8	13.5	7.6	n.g.
La ppm	19.8	26.4	4.5	19.1	13.0
Ce	41.0	55.1	9.8	45.0	24.3
Pr	4.45	5.87	1.07	6.70	4.43
Nd	16.9	21.5	3.85	27.4	22.9
Sm	3.40	4.29	1.26	8.40	8.40
Eu	0.621	0.712	0.174	0.090	0.040
LREE	86.198	113.928	20.636	106.690	73.068
Gd ppm	3.23	4.09	1.44	7.80	11.60
Tb	0.57	0.63	0.34	2.00	3.02
Dy	3.13	3.25	1.66	13.70	22.20
Ho	0.59	0.61	0.25	2.55	4.82
Er	1.60	1.66	0.63	7.72	17.30
Tm	0.233	0.221	0.102	1.40	3.06
Yb	1.39	1.28	0.67	9.10	20.90
Lu	0.196	0.182	0.096	1.23	3.16
HREE	10.951	11.914	5.189	45.55	86.06
L/HREE	7.9	9.6	4.0	2.3	0.85

Gb, Main phase biotite granite of the western body; Ga, Aplitic dikelet.
The Naegi data from Ishihara and Murakami (2006) and
Ishihara and Matsuhisa (2004)

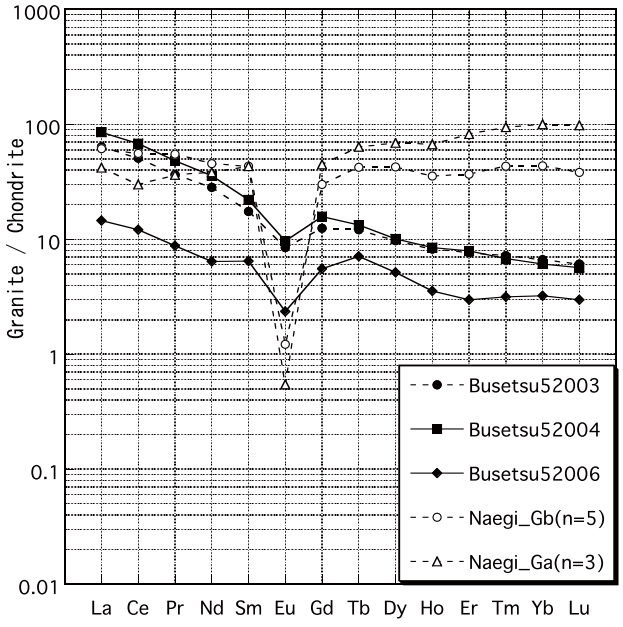

Fig. 14 Chondrite normalized REE patterns of the muscovite-biotite granites, Nakane- Sekizai quarry.

layering resulted from a flow differentiation that occurred at an interface of successive magma pulses, which cannot be applied to those of the Nakane-Sekizai quarry.

6. S-type vs. I-type granitoids: Genetic consideration

The studied granitoids are all reduced, belonging to ilmenite series (Ishihara, 1979), which has been considered due to supracrustal contamination of sedimentary carbon, based upon oxygen and sulfur isotopic studies (Ishihara and Matsuhisa, 2002; Ishihara and Sasaki, 2002). Within the ilmenite-series category, major compositions vary from south to north. The average silica contents, for example, are 60.1 % in the granitoids of the Zone I, but 75.2 % in those of the Zone VI, except for felsic granites of the Zone II (Table 2).

The granitoids of the Zone II are felsic, because of the presence of the muscovite-biotite granites of the Busetsu Granite, which are most close to the S-type of Chappell and White (1974). The granites contain no cordierite but muscovite and trace amounts of garnet as peraluminous minerals. The A/CNK ratio is generally higher than 1.1 (Nakai *et al.*, 1985; also Fig. 6B). Mafic enclaves are very rare, but small restitic sedi

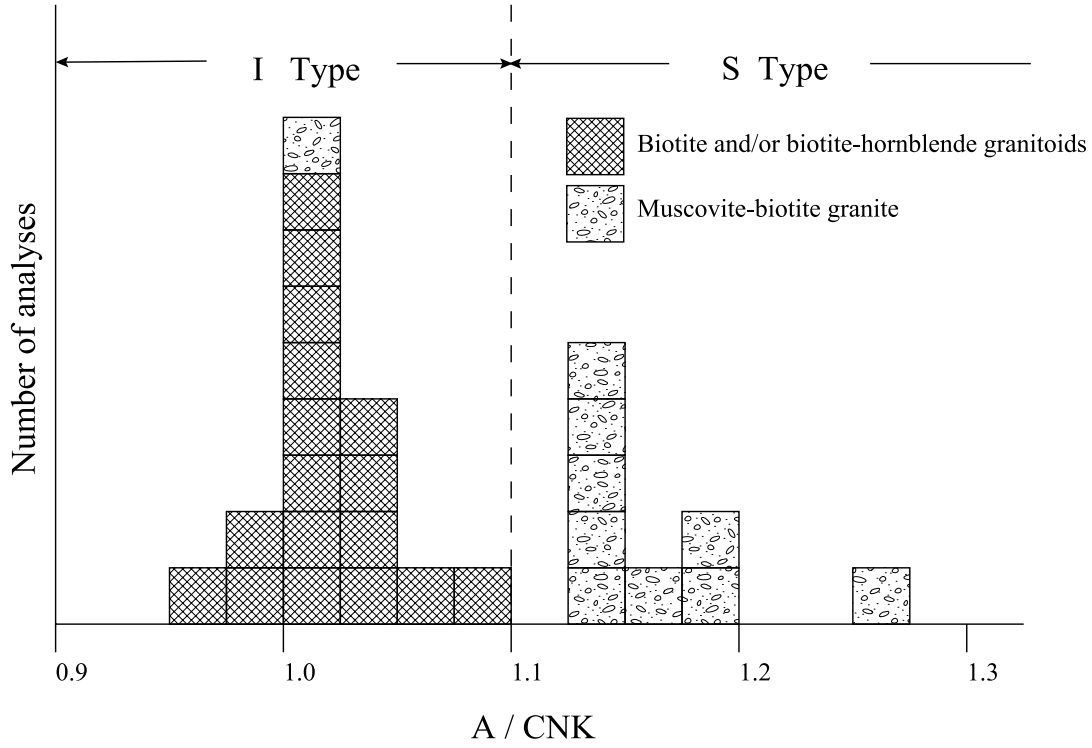

Fig. 15 Histograms of A/CNK ratio of the muscovite-biotite granite (Busetsu) and biotite granite of the Sanagesan-Obara and Seto Zones. 66T173A and B are averaged.

mentary fragments are sometimes observed (e.g., Figs. 3C, 13). The K_2O contents are not enough to define to the S-type, being generally below 4.5 %, and the Na_2O contents are higher than 2.3 % at 3 % K_2O. Therefore, the muscovite-biotite granites are quite different from the typical S-type in the Lachlan Fold Belt. Towards the northeast of the studied region, sillimanite was reported in the Ohtagiri muscovite-biotite granite (Katada and Murayama, 1961) and sillimanite and Zn-spinel were found in fine-grained aplitic granite at Tenryukyo by Tezuka (2005).

The major part of the studied granitoids have hornblende-biotite and/or biotite assemblage. The granitoids in the northern part, i,e, those of the Sanagesan-Obara zone and Seto zone, contain many biotite granites whose silica range is similar to that of the muscovite-biotite granite but contain only biotite as mafic silicate. Histograms of A/CNK ratio of these granites are shown in Fig.15. These granitoids are clearly separated by this ratio into two; the ratios of the muscovite-biotite granites are higher than 1.1 except for the 66T173 sample, but those of the biotite granites are below 1.1. Therefore the latter granitoids belong to I type.

The other major difference between the two types is P_2O_5 contents. An average of the muscovite-biotite granites is 0.105 % at 73.7 % SiO_2, but that of the biotite granites is lower than 0.021 % at 75.4 % SiO_2. In the Lachlan Fold Belt, the averaged S-type granite contains 0.15 % at 70.9 % SiO_2, whereas the averaged I-type granite is 0.11 % at 69.5 % SiO_2 (Chappell and White, 1992).

As mentioned previously, gabbroids occur sporadically but are dominant in the south. The granitoids are also mafic and calcic toward the same direction (Table 2). Blending mafic magmas from the upper mantle and felsic magmas generated within the continental crust by magma-mingling and mixing is an attractive idea to explain mafic I-type granitoids (Chappell, 1966), but occurrence of the gabbroids is so sporadic to explain a large distribution of quartz diorite to granodiorite. The I-type granitoids would reflect chemical compositions of the infracrustal source rocks (Chappell and Stephens, 1988).

The regional variation of MgO/Fe_2O_3 ratio in gabbroids mentioned previously would not possibly caused by magmatic differentiation but by different compositions in the source level. More abundant gabbroids in the south with MgO-rich character indicate that in-put of the gabbroic magmas from deep levels prevailed in the south. The gabbroic magmas should have also brought heat and volatiles from the upper mantle, which may have been the main heat source for the regional metamorphism of the Ryoke metamorphic belt. The heat also generated mafic granitic magmas in the infracrust, and even supracrust in the case of the Zone II, giving rise to the muscovite-

biotite granite of the Busetsu type. Thus, the felsic compositions of the Busetsu Granite is considered largely depending upon its felsic source rocks.

7. Relation to Mineralizations

One of the characteristics of the Ryoke granitoids is absence of metallic mineralizations among the ilmenite-series granitic activities of Southwest Japan, which is very clear as compared with the W-mineralized Naegi Granites of the Sanyo Belt (Ishihara and Murakami, 2006) to the north of the studied area. Intruded rocks are still preserved in the Shinshiro-Shitara zone, and the Busetsu Granite is felsic in composition and youngest in the intrusive sequence; yet these granitoids are almost barren except for small sizes of pegmatites, which may contain mineral species of molybdenite (Ishihara *et al*., 2002).

One of the reasons for the absence may be the depth of the granite formation. Depth of formation of the W-mineralized granites are considered to be 6 - 9 km (0.2 - 0.3 GPa) by the biotite geobarometer (Uchida *et al*., 2007). Ryoke metamorphism has been considered regional in scale, and intruded granitoids also emplaced in a deep level around the time of the metamorphism (Ishihara, 1973). Kutsukake (1997b) indeed estimated that crystallization of the Mitsuhashi pluton took place at the depth deeper than 15 km (～0.42 GPa). The Busetsu Granite may have intruded later into the Shimoyama tonalities but in a similar depth level.

The second reason for the lack of mineralization may be a low degree of magmatic fractionation, which is critical for concentration of volatiles and ore metals in the hydrothermal fluids. The Busetsu Granite is felsic having granitic composition and rich in water as shown by presence of muscovite, yet the Rb/Sr ratios are low ranging from 0.4 to 2.5 for the muscovite-biotite granite (see Nos. 17 - 27, Appendix). The highest No. 27 granite is muscovite-rich layer of Fig. 13 and depleted in the REE (Fig. 14). Their REE patterns are completely different from those of the well fractionated Naegi Granite with (Sn-)W mineralizations.

8. Concluding Remarks

Chemical compositions of the Ryoke granitoids were examined in the Chubu District. The granitoids are mostly I type and show a regional variation being mafic and calcic in the south, but become felsic toward the north. This regional variation was considered mostly due to chemical heterogeneity of the underlying continental crust where these magmas were generated. S-type granites were formed along the Zone II where the highest heat-flow was provided from the upper mantle to the supracrustal level. A little magmatic differentiation can be expected on these granitic activities.

Acknowledgements:The author thanks Prof. T. Kutsukake for reading of the original manuscript and Dr. Yutaka Takahashi for reviewing of the manuscript. Technical assistance of Ms. H. Shimizu is also acknowledged.

References

Chappell, B.W. (1966) Magma mingling and the production of compositional variation within granite suites: evidence from the granites of southeastern Australia. *Jour. Petrol*., **37**, 449-470.

Chappell, B. W. and Stephens, W. E. (1988) Origin of infracrustal (I-type) granite magmas. *Trans. Royal Soc. Edingburgh: Earth Sci*., **79**, 71-86.

Chappell, B. W. and White, A. J. R. (1974) Two contrasting granite types. *Pacific Geol*., no. 8, 173-174.

Chappell, B. W. and White, A. J. R. (1992) I- and S-type granites in the Lachlan Fold Belt. *Trans. Royal Soc. Edinburgh: Earth Sci*., **83**, 1-26.

Heckel, J. and Ryon, R. W. (2002) Polarized beam X-ray fluorescence analysis. *In* R. van Gricken and A. A. Markoiwicz eited. *Handbook of X-Ray Spectrometry, 2nd ed*., 603-630, Marcel Dekker, Inc.

Ishihara, S. (1971) Modal and chemical compositions of the granitic rocks related to the major molybdenum and tungsten deposits in the Inner Zone of Southwest Japan. *Jour. Geol. Soc. Japan*, **77,** 441-452.

Ishihara, S. (1973) The Mo-W metallogenic provinces and the related granitic provinces in Japan. *Mining Geology*, 23, 13-33 (in Japanese with English abstract).

Ishihara, S. (1978) Metallogenesis of the Japanese Island Arc system. *Jour. Geol. Soc. London*, **135**, 389-406.

Ishihara, S. (1979) Lateral variation of magnetic susceptibility of the Japanese granitoids. *Jour. Geol. Soc. Japan*, **85**, 509-523.

Ishihara, S. (2002) Chemical characteristics of the mineralized granitoids (I): Mo and W provinces of the Inner Zone of Southwest Japan. *Bull. Geol. Surv. Japan*, **53,** 657-672 (in Japanese with English abstract).

Ishihara, S. and Matsuhisa, Y. (2002) Oxygen isotopic constraints on the geneses of the Cretaceous-Paleogene granitoids in the Inner Zone of Southwest Japan. *Bull.Geol. Surv. Japan*, **53,** 421-438.

Ishihara, S. and Murakami, H. (2006) Fractionated ilmenite-series granites in Southwest Japan: Source magma for REE-Sn-W mineralizations. *Resource Geology*, **56,** 245-256.

Ishihara, S. and Sasaki, A. (2002) Paired sulfur isotopic belts: Late Cretaceous- Paleogene ore deposits in the Inner Zone of Southwest Japan. *Bull. Geol. Surv. Japan*, **53**, 461-477.

Ishihara, S. and Terashima, S. (1977) Chemical variation of the Cretaceous granitoids across southwestern Japan

— Shirakawa-Toki-Okazaki transaction. *Jour. Geol. Soc. Japan*, **83**, 327-339.

Ishihara, S. and Wu Chengyu (2001) Genesis of Late Cretaceous-Paleogene granitoids with contrasting chemical trend in the Chubu District, Central Japan. *Bull. Geol. Surv. Japan*, **52,** 471-491.

Ishihara, S., Jin, M. S. and Terashima, S. (2005) Mo-related adakitic granitoids from non-island-arc setting: Jecheon pluton of South Korea. *Resource Geol.*, **55**, 385-396.

Ishihara, S., Stein, H. J. and Tanaka, R. (2002) Re-Os age of molybdenite from the Busetsu two-mica granite, central Japan. *Bull. Geol. Surv. Japan*, **53**, 479-482.

Ishihara, S., Sekine, S., Mochizuki, T. and Oba, K. (1969) Contents of uranium and thorium in granitic rocks and their petrogenetic significance. *In* Natural Occurrence of Uranium in Japan, Part 2. *Rept. Geol. Surv. Japan*, no. 232, 179-220 (in Japanese with English abstract).

Kagashima, S. (1999) Layered structure in the Iwafune Granite, northeastern Japan and its isochron age. *Mem. Geol. Soc. Japan*, no. 53, 261-268.

Katada, M. and Murayama, M. (1961) Sillimanite-garnet bearing fine-grained granite (Otagiri Granite) exposed at the east of Kisokoma-gatake. *Bull. Geol. Surv. Japan*, **12**, 167-176 (in Japanese with English abstract).

Koide, H. (1958) Dando granodioritic intrusives and their associated metamorphic rocks. *Japan Society for the Promotion of Science, Tokyo*, 311 p.

Kutsukake, T. (1975) Metabasites in the Ryoke zone of the Toyone-mura area, Aichi Prefecture, Japan. *Jour. Japan. Assoc. Min. Petr. Econ. Geol.*, **70,** 177-193.

Kutsukake, T. (1993) An allanite-almandine-ferropargasite-annite selvage in the Mitsuhashi Granite in the Ryoke Belt, southwest Japan. *Earth Science*, **47**, 455-461.

Kutsukake, T. (1997a) Petrology and geochemistry of a calcic and ferrous granitoid pluton: the Mitsuhashi Granite in the Ryoke Belt, southwest Japan. *Jour. Min. Petr. Econ. Geol.*, **92**, 231-244.

Kutsukake, T. (1997b) The depth of emplacement of Mitsuhashi Granite pluton in the Ryoke Belt, southwest Japan — as inferred from some geobarometric calibrations. *Jour. Geol. Soc. Japan*, **103**, 604-607.

Kutsukake, T. (1997c) Garnet versus cummingtonite in quartz diorites of the Mitsuhashi Granite pluton in the Ryoke Belt, southwest Japan. *Earth Sci.*, **51**, 433-441.

Kutsukake, T. (2000) Petrographic features of the gabbroic rocks in the Ryoke Belt of the Mikawa district, southwest Japan. *Sci. Rept. Toyohashi Museum, Nat. Hist.*, **10**, 1-12.

Kutsukake, T. (2001) Geochemistry of the Kiyasaki Granodiorites in the Ryoke Belt, central Japan. *Sci. Rept. Toyohashi Museum, Nat. Hist.*, **11**, 1-12.

Linnenn, R. L. and Keppler, H. (2002) Melt composition control of Zr/Hf fractionation in magmatic processes. *Geochim. Cosmochim. Acta*, **66**, 3293-3301.

Makimoto, H., Yamada, N., Mizuno, K., Takada, A., Komazawa, M. and Sudo, S. (2004) Geological map of Japan 1:200,000, Toyohashi and Irago Misaki, Geol. Surv. Japan.

Nakai, Y. (1990) Granites of the Ryoke Belt. *In* Chubu District II, Geology of Japan, Kyoritsu Publishing Co., Tokyo, 97-99 (in Japanese).

Nakai, Y. and Suzuki, K. (2003) Post-tectonic two-mica granite in the Okazaki area, central Japan: a field guide for the 2003 Hutton Symposium. *Hutton Sym.-V Field Guidebook, Geol. Surv. Japan, Interim-Rept*. no. 28, 115-124.

Nakai, Y., Takeuchi, S., Suganuma, T., Ohta, S, Sakamoto, E., Yamamoto, N. and Uchida, Y. (1985) Formation history of geology and geography of the Okazaki City. *History of Okazaki City, Nature*, no. 14, 209 p. (in Japanese).

Nakajima, T., Kamiyama, H., Williams, I. S. and Tani, K.. (2004) Mafic rocks from the Ryoke Belt, southwest Japan: implications for Cretaceous Ryoke/San-yo granitic magma genesis. *Trans. Royal Soc. Edinburgh: Earth Sci.*, **95,** 249-263.

Tezuka, T. (2005) Fine granite with sillimanite found in Tenryukyo within the south of Kakasu zoned pluton in the Ryoke Belt, central Japan. *Natural History Rept. Inadani, Iida City Museum*, **6**, 47-48. (in Japanese).

Uchida, E., Endo, S. and Makino, M. (2007) Relationship between solidification depth of granitic rocks and formation of hydrothermal ore deposits. *Resource Geology*, **57**, 47-56.

Watson, E. B. and Harrison, T. M. (1983) Zircon saturation revisited: temperature and composition effects in a variety of crustal magma types. *Earth Planet. Sci. Let.*, **64**, 295-304.

Received August 14, 2007
Accepted November 1, 2007

中部地方の後期白亜紀領家帯花崗岩類の化学的性質の再検討

石原舜三・Bruce W. Chappell

要　旨

中部地方の領家帯において後期白亜紀の斑れい岩類（メタベイサイト）6試料，花崗岩類75試料の化学的性質の再検討を偏光蛍光X線分析法で実施した．花崗岩類の分析結果はＩタイプとＳタイプに2大別することができる．Ｉタイプの地帯別平均値を中央構造線から北方へ比較すると，新城 - 設楽帯（平均SiO_2含有量60.1 %），足助帯（同64.2 %），豊田 - 明智帯（同 70.0 %），猿投山 - 小原帯（同 73.0 %），瀬戸帯（同 75.2 %）と，北方へ珪長質となる．その原因はマグマの結晶分化作用よりも発生源である地殻中下部のinfracrustalな起源物質の相違を反映したものである．斑れい岩類は南部にやや卓越し，花崗岩類との混交現象も見られるが局在的で，恐らくマントルからの熱の運搬媒体として重要であったと思われる．

岡崎 - 武節帯の柘榴石含有白雲母黒雲母花崗岩（武節花崗岩）はアルミナ飽和度（A/CNK）上はＳタイプに属するが，アルカリ比についてはＩタイプである固有の性格を持っている．この岩体は領家変成岩類の高変成帯に貫入することから，高熱流量下でsupracrustalな大陸地殻まで溶融温度が達したために生じたものと考察された．領家変成帯南部にはルーフ岩石が残っているが鉱床は存在しない．その原因はその固結場所が15 kmに達するほど深かったため，及び武節花崗岩では珪長質ではあるがマグマ分化度が低かったために鉱化成分を含む熱水が発生・循環しなかったためと思われる．

Appendix: Chemical compositions of the studied granitoids from the Ryoke Belt.

	Shinshiro pluton			Shimoyama pluton				Mitsuhashi pluton				
	1	2	3	4	5	6	7	8	9	10	11	12
	RG37	RG38	RG39	65T78	65T79	66T151	66T134	RG10	RG06	RG07	RG08	RG09
SiO_2wt.%	51.06	58.43	60.22	61.32	60.83	60.76	60.35	47.80	51.55	62.58	71.13	75.33
TiO_2	1.28	0.94	0.86	0.72	0.79	0.80	0.81	1.59	1.04	0.70	0.31	0.06
Al_2O_3	17.42	16.19	16.32	15.59	15.80	15.89	16.83	18.64	16.30	16.11	14.56	13.48
Fe_2O_3	11.23	7.94	7.26	6.09	6.56	6.52	6.63	12.55	10.19	5.76	3.16	0.91
(FeO)	10.11	7.15	6.53	5.48	5.91	5.87	5.67	11.30	9.19	5.19	2.84	0.82
MnO	0.20	0.14	0.13	0.10	0.11	0.11	0.12	0.20	0.20	0.09	0.05	0.02
MgO	4.93	3.23	2.82	3.80	3.63	3.55	2.80	4.09	5.65	2.68	0.61	0.16
CaO	9.06	6.69	6.30	5.44	5.74	5.86	5.68	10.03	7.91	5.05	2.84	1.70
Na_2O	2.01	3.12	3.15	3.13	3.12	3.11	3.38	3.07	3.62	3.69	3.91	3.38
K_2O	1.01	1.52	1.61	2.41	2.25	2.36	2.32	1.16	2.54	2.24	2.69	4.04
P_2O_5	0.24	0.21	0.17	0.16	0.16	0.18	0.20	0.31	0.23	0.18	0.09	<0.01
S	0.07	0.01	0.01	0.03	0.04	0.06	0.01	0.07	0.09	0.03	0.01	<0.01
H_2O^+	1.21	1.39	0.95	0.99	0.95	0.84	0.68	0.95	0.96	0.93	0.47	0.42
H_2O^-	n.d.	n.d.	n.d.	n. d.	0.26	0.16	n. d.	0.12	0.06	0.04	0.08	0.29
CO_2	n.d.	n.d.	n.d.	n. d.	0.04	0.03	n. d.	0.14	0.14	0.15	0.10	0.09
Sum	99.67	99.80	99.80	99.75	100.26	100.20	99.79	100.68	100.43	100.22	100.01	99.87
Rb ppm	33	40	45	80	76	79	75	36	96	85	78	79
Cs	2.2	2.8	3.4	7.9	4.0	5.2	5.8	1.1	4.2	5.5	6.3	5.9
Sr	391	382	396	406	317	305	310	434	329	322	219	180
Ba	242	487	452	1010	463	520	560	207	428	479	830	840
Zr	53	124	102	143	120	155	127	169	187	131	139	21
Hf	2.2	3.7	3.5	3.7	3.8	4.5	3.2	6.0	5.8	4.7	4.9	2.0
Nb	8.2	8	7.5	10.1	10.9	12.2	10.4	13.5	16.7	12.4	12.3	4.4
Ta	4.8	3.4	< 2.2	< 2.0	2.4	< 2.7	2.1	3.3	5.3	3.9	1.8	< 1.4
Y	28	23	20	14	20	28	23	43	48	21	12	5
La	15	10	9	36	23	18	25	19	24	16	34	4
Ce	37	29	24	74	49	44	52	59	69	39	71	4
V	210	128	118	6	142	137	125	203	172	112	19	<2
Cr	78	15	14	33	131	99	57	12	228	65	15	9
Co	27	18	11	4	19	23	17	32	37	17	5	4
Ni	5	3	4	2	26	21	11	<2	54	13	<1	<1
Cu	8	6	6	< 0.5	17	16	5	16	39	11	1	1
Zn	113	93	87	35	74	71	70	117	115	70	92	30
Pb	6	8	10	27	10	10	13	8	10	12	16	27
Ga	18	19	19	16.9	17.7	18.7	16.4	21.0	18.9	18.4	20.1	13.9
Ge	1.6	1.3	1.6	1.1	1.3	1.5	1.4	1.5	1.7	1.4	1.0	1.3
As	< 0.4	0.5	0.5	< 0.3	0.5	0.7	0.6	< 0.4	< 0.4	< 0.4	< 0.4	< 0.5
Se	< 0.2	< 0.1	0.10	< 0.2	0.2	0.1	< 0.1	< 0.2	< 0.2	0.2	0.2	0.3
Mo	1.4	0.5	0.5	1.3	1.7	1.4	1.4	0.7	2.3	1.3	1.0	0.2
W	< 1.7	< 1.5	< 1.4	< 1.0	< 1.4	< 1.4	< 1.3	< 1.8	< 1.9	< 1.3	1.2	1.1
Sn	1.6	0.3	0.7	1.0	1.3	1.8	1.9	1.1	1.5	1.1	1.3	1.6
Cd	0.7	0.2	0.2	< 0.2	0.3	0.4	< 0.2	0.4	0.2	0.3	< 0.2	0.6
Tl	< 0.6	0.3	0.5	< 0.7	< 0.5	0.4	0.5	< 0.7	0.4	0.9	0.7	1.3
Th	3.7	2	1.6	7.1	9.1	4.8	10.9	1.5	1.8	4.9	9.9	2.8
U	0.8	0.6	1.4	< 0.5	1.4	2.0	2.4	1.4	1.1	1.6	0.7	1.3
A/CNK	0.84	0.86	0.89	0.88	0.88	0.86	0.92	0.76	0.71	1.11	1.02	1.04
NK/A	0.25	0.42	0.42	0.50	0.48	0.48	0.48	0.34	0.53	0.53	0.64	0.74
Fe_2O_3/ MgO	2.28	2.46	2.58	1.60	1.81	1.84	2.37	3.07	1.80	2.15	5.14	5.83
Ga*10000/A	2.0	2.3	2.2	2.0	2.1	2.2	1.8	2.1	2.2	2.2	2.6	1.9
Rb/Sr	0.1	0.1	0.1	0.2	0.2	0.3	0.2	0.1	0.3	0.3	0.4	0.4
Sr/Y	14.0	16.6	19.8	29.0	15.9	10.9	13.5	10.1	6.9	15.3	18.3	36.0
Zr-T(˚C)	647	723	716	744	728	746	736	701	710	741	768	636

Appendix: Continued.

	Ure pluton			Okazaki-Busetsu zone								
	13	14	15	16	17	18	19	20	21	22	23	24
	RG32	RG31	RG33	65T76	65T81	66T133	66T135	66T136	66T173A	66T173B	52002	52003
SiO_2wt.%	48.83	56.07	73.60	71.52	74.97	74.83	70.92	75.31	69.35	73.44	74.85	73.15
TiO_2	1.88	1.46	0.14	0.21	0.12	0.09	0.28	0.10	0.43	0.14	0.11	0.15
Al_2O_3	17.22	16.96	13.69	16.53	13.61	13.63	15.14	13.56	14.19	13.81	14.21	14.75
Fe_2O_3	12.03	10.10	1.87	1.96	1.37	1.09	2.94	1.18	3.78	1.46	1.30	1.90
(FeO)	10.83	9.09	1.68	1.90	1.04	0.86	2.44	1.19	1.90	1.19	n.d.	n.d.
MnO	0.21	0.14	0.05	0.03	0.04	0.05	0.07	0.04	0.07	0.03	0.04	0.06
MgO	3.12	2.42	0.22	0.54	0.26	0.22	0.64	0.27	1.08	0.35	0.27	0.37
CaO	8.67	6.02	1.69	2.66	1.26	1.05	3.09	1.33	3.49	1.30	1.33	1.62
Na_2O	4.03	3.16	3.04	3.33	3.10	2.91	3.76	3.24	2.52	2.48	3.51	3.94
K_2O	2.20	2.04	5.00	2.65	4.17	4.46	2.06	3.81	4.35	6.01	3.95	3.15
P_2O_5	0.43	0.42	0.03	0.08	0.09	0.11	0.12	0.07	0.06	0.12	0.08	0.11
S	0.02	0.05	<0.01	<0.01	<0.01	<0.01	<0.01	<0.01	<0.01	<0.01	<0.01	<0.01
H_2O^+	1.06	0.88	0.61	0.49	0.57	0.49	0.74	0.63	0.46	0.14	0.34	0.63
H_2O^-	-0.01	-0.02	n.d.	0.14	0.32	0.20	0.30	0.34	0.26	0.50	0.16	0.15
CO_2	n.d.	n.d.	n.d.	0.03	0.01	0.81	0.01	0.00	0.03	0.02	0.01	0.01
Sum	99.69	99.68	99.94	102.07	99.89	100.80	100.07	99.88	101.97	100.99	100.16	99.99
Rb ppm	50	58	134	67	124	192	58	117	106	123	123	132
Cs	2.5	2.2	7.5	4.5	5.3	6.6	4.3	5.2	6.9	11.7	n.d.	n.d.
Sr	445	481	162	408	188	87	381	197	239	298	214	201
Ba	850	760	680	882	718	214	502	806	853	1679	600	482
Zr	389	356	112	160	79	50	127	70	105	103	73	103
Hf	8.4	8.5	4.8	5	4	3	4	3	5	4	3.1	4.3
Nb	16.7	15.3	9.6	9.7	10.1	9.6	8.7	10	8.2	7.4	10.7	15.1
Ta	3.7	2.8	4	1	2	2	1	3	3	3	n.d.	n.d.
Y	56	22	16	12	14	17	14	14	49	12	17	17
La	101	88	23	28	20	9	23	25	18	26	20	16
Ce	183	168	44	57	42	21	46	49	48	55	39	33
V	130	95	3	12	4	8	20	4	43	7	<3	<3
Cr	<1	<1	4	30	4	8	6	4	11	3	25	30
Co	29	17	5	7	3	4	6	4	14	4	n.d.	n.d.
Ni	<1	<1	<1	3	1	1	< 0.7	1	< 0.8	< 0.6	1	1
Cu	10	11	< 0.4	< 0.4	1	< 0.3	< 0.4	< 0.4	< 0.4	< 0.4	<0.4	<0.4
Zn	110	116	43	57	44	33	67	39	51	41	45	64
Pb	9	10	35	20.1	28.1	27.3	18	22.9	24.9	35.4	27	22
Ga	23.6	23	16.4	16.2	16.4	16.4	17.8	18	14.5	14.2	17.6	20.3
Ge	1.4	1.7	1.4	1	1.4	1.9	1.7	1.5	1.5	1	n.d.	n.d.
As	< 0.4	< 0.4	< 0.6	< 0.4	0.5	< 0.5	< 0.4	< 0.4	< 0.5	< 0.6	0.4	<0.5
Se	< 0.2	< 0.2	0.2	0.2	< 0.1	0.2	0.2	0.2	< 0.1	0.2	n.d.	n.d.
Mo	1.1	1.4	< 0.2	0.6	< 0.2	< 0.2	< 0.2	< 0.2	0.3	0.4	<0.2	<0.2
W	< 1.8	< 1.6	0.3	0.8	1.7	1.2	0.7	1.1	0.7	0.6	n.d.	n.d.
Sn	1.5	< 0.4	2.8	0.6	1.6	4.1	2.1	1.9	2.4	1.4	1.2	1.7
Cd	0.5	< 0.2	< 0.2	0.2	< 0.2	< 0.2	< 0.2	0.4	0.4	0.5	<0.2	<0.2
Tl	< 0.6	0.5	1.2	1.1	1.1	1.3	0.6	1	1	1.3	1.1	1
Th	21	21.9	15.4	8	6.2	3.4	3.9	6.6	12.9	8.8	6	4.1
U	1	0.9	4.6	1.5	1.4	2.3	0.5	< 0.5	6.2	< 0.5	1.6	1.2
A/CNK	0.70	0.92	1.02	1.25	1.14	1.18	1.08	1.14	0.93	1.07	1.14	1.15
NK/A	0.52	0.44	0.76	0.50	0.71	0.71	0.56	0.70	0.62	0.77	0.71	0.67
Fe_2O_3/ MgO	3.85	4.18	8.40	3.65	5.27	4.92	4.63	4.43	3.50	4.19	4.81	5.14
Ga*10000/A	2.6	2.6	2.3	1.9	2.3	2.3	2.2	2.5	1.9	1.9	2.3	2.6
Rb/Sr	0.1	0.1	0.8	0.2	0.7	2.2	0.2	0.6	0.4	0.4	0.6	0.7
Sr/Y	7.9	21.9	10.1	34.0	13.4	5.1	27.2	14.1	4.9	24.8	12.6	11.8
Zr-T(˚C)	754	821	755	802	739	707	768	730	736	753	732	759

Appendix: Continued.

	Okazaki-Busetsu zone											
	25	26	27	28	29	30	31	32	33	34	35	36
	52004	52005	52006	RG26	RG28	RG27	RG29	RG30	RG36	RG35	66T165	66T168
SiO_2wt.%	74.50	74.45	74.84	51.33	71.36	76.36	57.20	70.39	55.06	72.25	51.87	68.48
TiO_2	0.13	0.10	0.03	1.81	0.25	0.05	1.58	0.39	1.87	0.21	2.05	0.46
Al_2O_3	14.29	14.35	14.61	17.59	14.62	13.11	16.46	13.38	16.73	13.72	17.15	14.68
Fe_2O_3	1.55	1.20	0.51	11.91	2.97	0.85	10.29	4.14	10.52	2.43	12.19	4.12
(FeO)	n.d.	n.d.	n.d.	10.72	2.67	0.77	9.26	3.73	9.47	2.19	10.97	3.71
MnO	0.05	0.03	0.04	0.19	0.06	0.01	0.17	0.07	0.16	0.04	0.21	0.08
MgO	0.31	0.25	0.09	3.03	0.39	0.09	1.71	0.68	2.57	0.33	3.29	1.17
CaO	1.53	1.38	0.71	8.86	2.12	1.49	6.75	2.74	7.57	2.07	8.28	3.55
Na_2O	3.65	3.60	3.87	2.75	2.81	2.26	2.55	3.10	2.92	3.78	2.78	2.48
K_2O	3.57	3.92	4.37	1.01	4.56	5.30	1.94	3.64	1.43	4.50	1.55	4.37
P_2O_5	0.10	0.09	0.21	0.45	0.13	0.03	0.38	0.10	0.41	0.06	0.31	0.07
S	<0.01	<0.01	<0.01	0.04	<0.01	<0.01	0.02	0.02	0.02	<0.01	0.04	0.01
H_2O^+	0.56	0.35	0.55	0.77	0.75	0.29	0.70	1.11	0.71	0.39	0.62	0.16
H_2O^-	-0.39	0.15	0.08	-0.02	n.d.	n.d.	-0.01	-0.01	-0.01	n.d.	0.52	0.46
CO_2	0.09	0.04	0.01	n.d.	n.d.	n.d.	n.d.	n.d.	n.d.	n.d.	0.06	0.02
Sum	99.94	99.91	99.92	99.72	100.02	99.85	99.73	99.75	99.97	99.78	100.91	100.1
Rb ppm	118	120	164	25	131	101	49	70	39	150	42	112
Cs	n.d.	n.d.	n.d.	< 1.5	7.7	1.9	1.7	4.2	1.4	7.6	2.3	9.8
Sr	234	219	65	374	185	109	346	227	399	198	357	246
Ba	689	592	105	352	570	203	720	750	510	760	341	820
Zr	89	71	21	233	113	57	231	142	250	115	171	89
Hf	3.2	3.2	1.8	6.5	5.3	4	7	5.5	7.9	4.8	4	4.7
Nb	11.7	10	9.7	15.2	9.8	2.5	17.4	8.5	17.2	11	15.2	8.6
Ta	n.d.	n.d.	n.d.	< 2.8	3.7	2	4	1.8	< 3.4	2.4	< 3.2	1.9
Y	17	16	9	44	25	9	43	18	41	12	40	46
La	18	16	3	19	16	3	21	24	14	24	18.0	8.0
Ce	41	34	6	51	37	11	53	53	47	52	54	24
V	2	<3	<1	145	14	<2	108	30	132	8	109	43
Cr	21	28	25	<1	2	1	<1	5	<1	2	40	9
Co	n.d.	n.d.	n.d.	23	9	4	25	7	28	4	17	12
Ni	1	1	1	<1	<1	<1	<1	<1	<1	<1	2	<1
Cu	<0.4	<0.4	<0.3	9	< 0.4	< 0.3	8	< 0.4	25	< 0.4	18	< 0.4
Zn	54	41	22	126	50	13	124	57	122	36	125	55
Pb	26	26	20	6	26	33	8	18	6	36	7	26
Ga	18	18	20.2	22.1	17.1	13.3	21.9	15.9	21	18.4	21.3	15.6
Ge	n.d.	n.d.	n.d.	1.4	1.6	1.4	1.4	0.9	1.7	1.5	1.6	1.6
As	<0.5	<0.5	0.2	< 0.4	< 0.5	< 0.5	< 0.4	0.3	< 0.4	< 0.6	0.4	< 0.5
Se	n.d.	n.d.	<0.2	< 0.2	0.2	< 0.1	0.1	0.5	< 0.2	0.2	< 0.2	< 0.1
Mo	<0.2	<0.2	<0.2	1.8	0.3	< 0.2	2.1	0.5	1.6	1	1.5	0.3
W	n.d.	n.d.	n.d.	< 1.8	< 1.1	1.7	< 1.7	1.6	< 1.7	1.1	< 1.8	0.7
Sn	1.4	1.1	1.5	0.5	2	0.6	0.8	1.3	0.5	3.3	< 0.4	2.5
Cd	<0.2	<0.2	0.2	0.2	< 0.2	0.2	0.3	0.6	0.7	0.2	0.3	0.3
Tl	1.3	1.4	1.3	< 0.6	1.6	1.3	0.8	1.8	< 0.6	1.3	< 0.6	0.8
Th	7	5.1	< 0.5	5.2	11.7	2.4	4.7	12.1	2.1	11	1.5	7.2
U	< 0.5	< 0.5	1.3	0.9	4	1.7	0.6	1.3	1.4	4.4	1	3
A/CNK	1.13	1.13	1.18	0.81	1.01	1.08	0.89	0.95	0.83	0.96	0.81	0.96
NK/A	0.69	0.71	0.76	0.32	0.65	0.72	0.38	0.68	0.38	0.81	0.37	0.60
Fe_2O_3/ MgO	5.00	4.80	5.67	3.93	7.62	9.22	6.02	6.09	4.10	7.42	3.71	3.53
Ga*10000/A	2.4	2.4	2.6	2.4	2.2	1.9	2.5	2.2	2.4	2.5	2.3	2.0
Rb/Sr	0.5	0.6	2.5	0.1	0.7	0.9	0.1	0.3	0.1	0.8	0.1	0.5
Sr/Y	13.8	13.7	7.2	8.5	7.4	12.1	8.0	12.6	9.7	16.5	8.9	5.3
Zr-T(˚C)	747	729	645	750	761	710	778	766	769	745	727	726

Appendix: Continued.

	Asuke zone											
	37	38	39	40	41	42	43	44	45	46	47	48
	66T167	RG22	RG23	RG24	RG25	65T74	65T75	SJ10	SJ11	66T131	66T130	65T71
SiO_2wt.%	72.72	59.93	57.53	59.19	57.92	65.36	66.58	64.68	72.16	66.68	70.99	69.72
TiO_2	0.28	1.14	1.22	0.87	1.20	0.70	0.58	0.65	0.33	0.35	0.40	0.36
Al_2O_3	13.36	15.70	15.53	16.01	15.68	15.09	15.57	16.54	14.30	15.24	13.73	14.73
Fe_2O_3	2.61	8.44	9.00	7.35	7.83	5.78	4.94	5.29	2.49	3.58	3.35	3.15
(FeO)	2.35	7.60	8.10	6.62	7.05	5.20	4.45	n.d.	n.d.	3.22	3.02	2.84
MnO	0.05	0.15	0.16	0.14	0.14	0.10	0.07	0.08	0.04	0.08	0.06	0.05
MgO	0.75	1.83	2.35	1.98	2.33	1.70	1.15	1.31	0.59	0.85	0.84	0.80
CaO	2.76	6.39	6.38	6.87	6.86	4.70	4.42	4.77	3.18	3.87	2.99	3.88
Na_2O	2.22	2.52	3.66	3.67	3.30	2.82	3.44	3.57	3.19	4.83	2.89	3.17
K_2O	4.84	2.71	2.78	2.42	2.50	2.79	2.36	2.33	2.95	3.89	4.09	3.06
P_2O_5	0.04	0.24	0.24	0.19	0.26	0.13	0.13	0.15	0.08	0.14	0.08	0.08
S	<0.01	0.01	0.02	0.03	0.02	0.01	0.01	<0.01	0.01	0.01	0.02	0.02
H_2O^+	0.08	0.73	0.89	1.05	1.75	0.61	0.66	0.73	0.36	0.23	0.31	0.60
H_2O^-	0.24	n.d.	-0.01	-0.01	-0.01	n.d.	0.32	0.16	0.18	n.d.	-0.01	0.24
CO_2	0.01	n.d.	n.d.	n.d.	n.d.	n.d.	0.03	0.01	0.13	n.d.	n.d.	0.09
Sum	99.967	99.78	99.75	99.76	99.78	99.80	100.26	100.27	99.98	99.74	99.73	99.95
Rb ppm	100	124	135	105	126	105	80	82	76	84	102	83
Cs	9.8	4.0	3.2	6.1	5.0	5.4	5.1	n.d.	n.d.	5.4	6.5	7
Sr	236	262	235	284	264	265	282	311	277	285	221	285
Ba	1060	530	434	640	650	640	680	770	1050	465	1090	1150
Zr	68	125	140	119	147	137	186	190	167	107	110	187
Hf	3.3	4.9	5.4	2.6	2.4	5.1	5.3	4.9	6.2	2.5	4.1	4.3
Nb	4.9	10.6	11	12.3	10.9	10.5	11.5	12.7	6.4	10.8	7.8	6.3
Ta	2.2	4	3.4	2.7	< 2.4	2.6	2.6	n.d.	n.d.	< 2.0	< 1.9	1.6
Y	29	26	25	19	31	40	29	31	13	20	26	17
La	6.0	21	33	7	17	30	26	33	38	21	21	35
Ce	20	44	72	17	42	67	60	72	80	48	50	73
V	26	110	100	78	109	70	45	37	17	145	33	34
Cr	10	31	21	4	3	17	32	30	30	263	30	3
Co	9	17	19	14	16	13	8	n.d.	n.d.	20	9	8
Ni	<1	<1	<1	<1	<1	<1	3	<1	1	40	3	<1
Cu	< 0.4	5	2	2	7	3	4	5	< 0.4	14	5	8
Zn	35	95	108	87	95	72	66	75	40	69	49	52
Pb	26	9	10	10	9	15	11	11	14	10	16	17
Ga	12	18.8	18.7	19.6	20.5	18.4	20.4	22.1	16.1	17.6	15.1	17
Ge	1.2	1.2	1.3	1.6	1.4	1.8	1.2	n.d.	n.d.	1.5	1	1.3
As	< 0.5	< 0.4	< 0.4	< 0.4	< 0.4	< 0.4	0.6	< 0.4	< 0.4	0.3	0.4	1.1
Se	0.2	< 0.1	0.4	< 0.1	< 0.1	< 0.1	0.1	< 0.2	0.4	< 0.2	< 0.1	0.2
Mo	0.3	1.1	1.5	1.5	1.1	1.4	1.4	1.4	0.2	2	1.2	0.9
W	0.7	< 1.4	< 1.5	< 1.4	< 1.5	< 1.3	< 1.2	nd	nd	< 1.0	< 1.1	< 1.1
Sn	2.3	0.8	0.8	0.8	0.5	1.9	0.6	0.4	0.9	1.7	1.0	1.5
Cd	0.4	0.4	0.4	< 0.2	< 0.2	< 0.2	< 0.2	0.2	0.5	0.4	0.4	< 0.2
Tl	0.8	1.4	2	0.8	0.7	0.8	0.6	0.4	1.7	< 0.7	0.6	0.5
Th	5.8	5.7	10.5	1	4.3	11.6	7.4	8.3	13.6	8.7	6.7	13.1
U	1.9	0.9	1	1.3	0.5	0.6	0.7	1.3	0.6	1.3	1.7	1.6
A/CNK	0.96	0.84	0.75	0.76	0.76	0.93	0.96	0.97	1.01	0.79	0.94	0.95
NK/A	0.67	0.45	0.58	0.54	0.52	0.51	0.53	0.51	0.59	0.80	0.67	0.58
Fe_2O_3/ MgO	3.48	4.62	3.83	3.70	3.35	3.40	4.31	4.04	4.22	4.21	3.98	3.94
Ga*10000/A	1.7	2.3	2.3	2.3	2.5	2.3	2.5	2.5	2.1	2.2	2.1	2.2
Rb/Sr	0.4	0.5	0.6	0.4	0.5	0.4	0.3	0.3	0.3	0.3	0.5	0.3
Sr/Y	8.1	10.1	9.4	14.9	8.5	6.6	9.7	10.0	21.3	14.3	8.5	16.8
Zr-T(˚C)	710	724	712	701	718	753	782	781	785	710	743	785

Appendix: Continued.

	Toyota -Akechi zone											
	49	50	51	52	53	54	55	56	57	58	59	60
	65T72	SJ08	SJ09	66T114	66T120	FJK	66T117	66T128	66T118	66T129	66T127	55T126
SiO_2wt.%	73.81	69.33	69.19	75.73	76.71	65.47	68.02	64.79	66.66	68.26	69.54	70.87
TiO_2	0.17	0.29	0.31	0.08	0.10	0.39	0.28	0.60	0.59	0.26	0.35	0.24
Al_2O_3	13.35	16.04	15.86	12.39	12.49	18.11	16.89	15.67	14.73	16.91	15.21	15.26
Fe_2O_3	1.90	2.70	3.00	1.18	1.44	3.37	2.73	5.14	5.03	2.33	3.04	2.33
(FeO)	1.71	n.d.	n.d.	1.06	1.30	n.d.	2.46	4.63	4.53	2.10	2.74	2.10
MnO	0.04	0.04	0.05	0.02	0.06	0.05	0.04	0.10	0.09	0.04	0.05	0.03
MgO	0.27	0.42	0.48	0.14	0.19	0.60	0.51	1.92	1.80	0.45	0.81	0.34
CaO	2.15	3.84	3.82	1.49	0.77	5.37	4.61	5.21	4.52	4.66	4.00	3.32
Na_2O	2.39	3.39	3.42	2.78	3.40	3.78	3.52	3.13	2.77	3.17	3.10	3.84
K_2O	5.19	3.12	3.04	4.75	4.72	2.08	2.75	2.50	3.06	2.87	3.25	2.98
P_2O_5	0.04	0.09	0.10	<0.01	0.02	0.11	0.04	0.11	0.10	0.05	0.05	0.05
S	0.01	<0.01	<0.01	0.01	<0.01	<0.01	0.01	0.01	0.01	0.01	0.02	0.01
H_2O^+	0.44	0.47	0.44	0.87	-0.04	0.53	0.33	0.66	0.47	0.68	0.36	0.26
H_2O^-	n.d.	0.15	0.29	0.42	n.d.	0.13	n.d.	0.38	n.d.	0.22	-0.01	0.40
CO_2	n.d.	0.03	0.15	0.01	n.d.	0.08	n.d.	0.02	n.d.	0.04	n.d.	0.01
Sum	99.76	99.91	100.15	99.87	99.86	100.07	99.72	100.22	99.81	99.94	99.76	99.95
Rb ppm	111	70	74	115	137	70	75	97	101	76	101	69
Cs	7.2	n.d.	n.d.	4.8	5.9	n.d.	7.1	8.8	7.1	8.3	5.1	6.1
Sr	187	337	324	145	114	377	366	241	226	348	261	240
Ba	970	1550	1300	790	660	841	1350	270	455	1240	830	1040
Zr	101	194	208	82	97	223	152	109	77	197	121	213
Hf	2.1	5.3	5	4.1	4.7	6.6	3.8	3.2	2.6	4.9	2.8	5.2
Nb	5.4	6	7.3	3.9	6.8	9.6	6.6	7.1	7.2	6	6.4	7.4
Ta	< 1.6	n.d.	n.d.	1.8	2.4	n.d.	2.6	2.4	3	1	< 1.7	1.3
Y	10	18	22	16	21	23	19	22	20	16	20	17
La	26	44	46	29	25	65	56	23	10	34	32	20
Ce	52	84	94	50	54	122	109	41	21	67	66	47
V	10	14	13	3	8	13	23	63	60	20	28	15
Cr	45	28	21	3	29	25	99	11	60	2	39	1
Co	5	n.d.	n.d.	<3	<4	n.d.	6	14	10	9	7	6
Ni	6	1	1	1	4	1	12	4	7	<1	4	<1
Cu	1	< 0.4	0.4	< 0.4	< 0.4	3	1	2	1	< 0.4	2	1
Zn	27	44	47	24	36	53	43	62	57	38	51	37
Pb	19	14	14	22	23	13	16	20	19	15	27	17
Ga	13.7	17.8	17.8	12.6	13.7	21.6	19.1	17	15.7	18.4	15.8	18.6
Ge	1.2	n.d.	n.d.	1.2	1.4	n.d.	1	1.5	1.5	1	1.3	1.2
As	0.5	0.4	0.3	< 0.4	< 0.5	0.5	< 0.4	1.1	< 0.4	1.7	0.3	0.8
Se	< 0.1	0.2	n.d.	0.2	< 0.1	n.d.	0.2	< 0.1	< 0.1	< 0.1	< 0.1	< 0.1
Mo	1.5	1.7	1.2	< 0.2	3.8	2.1	2.3	0.7	1.3	0.3	1.9	0.4
W	0.7	nd	nd	1.2	0.9	n.d.	0.9	< 1.2	< 1.2	0.6	0.6	1.8
Sn	1.2	0.8	0.7	1.3	1.2	1	1.7	3.2	2.3	1.5	3.2	1.1
Cd	< 0.2	0.3	0.2	< 0.2	< 0.2	< 0.2	< 0.2	0.3	< 0.2	< 0.2	< 0.2	< 0.2
Tl	0.5	0.7	0.8	1.0	1.2	0.9	0.9	0.8	0.9	0.8	1.0	0.6
Th	9.7	11.4	12.8	11.2	13.3	16.6	15.4	12.5	4	12.2	14.2	6.1
U	1.0	1.9	1.1	1.5	2.8	0.9	0.6	2.7	2.1	1.6	1.7	1.1
A/CNK	0.99	1.01	1.00	1.00	1.03	0.99	0.99	0.90	0.92	1.01	0.96	0.98
NK/A	0.72	0.56	0.56	0.78	0.86	0.47	0.52	0.50	0.53	0.49	0.57	0.63
Fe_2O_3/ MgO	7.12	6.43	6.25	8.18	7.57	5.62	5.40	2.68	2.80	5.17	3.75	6.93
Ga*10000/A	1.9	2.1	2.1	1.9	2.1	2.3	2.1	2.1	2.0	2.1	2.0	2.3
Rb/Sr	0.6	0.2	0.2	0.8	1.2	0.2	0.2	0.4	0.5	0.2	0.4	0.3
Sr/Y	18.7	18.7	14.7	9.1	5.4	16.4	19.3	11.0	11.3	21.8	13.1	14.1
Zr-T(˚C)	745	793	798	732	749	795	766	729	707	791	749	800

Appendix: Continued.

		Sanagesan - Obara zone										
	61	62	63	64	65	66	67	68	69	70	71	72
	66T125	66T105	66T121	66T109	66T153	65T67	65T66	65T97	65T65	65T99	65T62	66T123
SiO_2wt.%	71.56	68.18	74.85	78.34	73.73	74.72	77.40	67.65	68.57	69.48	75.60	74.62
TiO_2	0.32	0.27	0.19	0.05	0.10	0.16	0.06	0.49	0.46	0.44	0.14	0.10
Al_2O_3	14.26	15.46	12.68	11.69	14.10	13.25	12.07	14.94	14.57	14.51	12.73	13.63
Fe_2O_3	2.69	2.73	2.12	0.77	1.53	2.05	1.25	4.12	4.08	3.95	1.60	1.21
(FeO)	2.42	2.46	1.91	0.69	1.38	1.85	1.13	3.71	3.67	3.56	1.44	1.09
MnO	0.04	0.07	0.08	0.03	0.06	0.04	0.03	0.08	0.09	0.09	0.02	0.02
MgO	0.41	0.66	0.41	0.13	0.21	0.27	0.11	1.28	1.41	1.03	0.18	0.15
CaO	3.63	2.37	1.35	1.00	1.64	1.55	1.18	3.89	3.88	3.52	1.62	1.06
Na_2O	3.29	3.16	3.32	2.93	3.90	3.03	2.47	3.07	2.88	2.26	2.79	3.51
K_2O	2.96	5.95	4.61	4.40	4.39	4.58	4.91	3.41	3.18	3.76	4.72	5.41
P_2O_5	0.06	0.05	0.04	<0.01	<0.01	0.02	<0.01	0.09	0.09	0.07	<0.01	<0.01
S	0.02	0.02	0.01	0.01	0.01	0.01	<0.01	0.01	0.01	0.01	0.01	<0.01
H_2O^+	0.49	0.48	0.18	0.27	0.17	0.36	0.34	0.67	0.62	0.93	0.37	0.33
H_2O^-	-0.01	0.36	n.d.	0.26	n.d.	n.d.	n.d.	0.38	n.d.	n.d.	n.d.	n.d.
CO_2	n.d.	0.23	n.d.	0.01	n.d.	n.d.	n.d.	0.06	n.d.	n.d.	n.d.	n.d.
Sum	99.71	99.97	99.83	99.88	99.84	100.03	99.82	100.15	99.8	100.04	99.78	100.04
Rb ppm	87	196	147	164	204	141	143	127	121	136	132	199
Cs	6.4	10.4	4.8	3.9	6.7	5.7	4.9	8.6	7.6	8.1	6.8	5.3
Sr	265	184	82	72	90	104	107	209	203	191	145	71
Ba	1220	1020	422	423	254	560	560	440	398	444	920	510
Zr	182	112	58	63	69	103	73	113	93	95	136	92
Hf	4.5	4.8	2.3	4.3	3.6	3.4	3.9	4.0	4.7	5.1	5	3.9
Nb	9.7	7.0	3.5	4.0	8	8.2	5.5	7.8	7.4	7.1	7	7.1
Ta	1.9	2.0	< 1.4	3.7	2.6	< 1.5	1.6	2.5	2.8	4.3	2.8	1.9
Y	25	32	17	25	37	15	21	31	29	26	22	34
La	48	15	16	8	17	34	22	25	25	23	52	34
Ce	93	37	28	26	33	75	47	54	51	48	98	68
V	3	32	5	2	6	10	<2	47	50	50	6	5
Cr	36	5	40	5	28	25	26	8	30	52	8	44
Co	8	11	4	4	7	<4	3	12	13	7	4	3
Ni	4	<1	3	<1	1	1	3	<1	2	5	2	3
Cu	3	< 0.4	< 0.3	< 0.4	< 0.4	< 0.4	< 0.4	< 0.4	1	1	1	< 0.4
Zn	47	46	24	19	31	42	28	54	54	53	32	26
Pb	16	31	25	30	31	25	24	23	24	28	23	24
Ga	17.1	15.8	11.6	12.1	16.1	14.4	13	16.1	15.8	14.5	14.9	16.9
Ge	1.2	1.6	1.3	1.3	1.7	1.1	1	1.5	1.4	1.8	1.4	1.5
As	1.2	< 0.5	< 0.5	< 0.5	< 0.5	< 0.5	< 0.5	0.6	< 0.5	< 0.5	0.8	< 0.5
Se	< 0.1	0.2	0.1	0.1	0.2	< 0.1	0.2	< 0.1	0.3	0.3	< 0.1	0.2
Mo	1.5	0.5	0.6	< 0.2	< 0.2	0.6	0.8	1.4	0.9	0.8	0.5	0.4
W	< 1.0	0.9	1.4	1.5	0.8	2.2	1.2	0.8	< 1.1	< 1.2	1.4	1.4
Sn	1.9	3.2	1.3	1.7	3.4	2	1.5	3.8	4.7	4.2	1.8	0.9
Cd	0.3	0.2	0.4	0.8	< 0.2	0.3	< 0.2	< 0.2	< 0.2	0.2	< 0.2	< 0.2
Tl	0.7	1.2	0.8	1.4	1.4	0.7	1.1	0.8	1.0	1.1	1.1	1.3
Th	9.2	11.2	9.2	20.1	18.2	14.6	13.9	16.1	14.9	13.5	15.8	13.2
U	1.3	2.9	2.9	2.6	7.7	2.7	2.1	3.7	< 0.5	1.7	1.9	2.1
A/CNK	1.19	0.97	0.98	1.03	1.00	1.04	1.05	0.95	0.96	1.02	1.01	1.01
NK/A	0.60	0.75	0.82	0.82	0.79	0.75	0.78	0.59	0.56	0.54	0.76	0.85
Fe_2O_3/ MgO	6.58	4.13	5.19	5.75	7.23	7.65	11.31	3.21	2.90	3.82	8.76	8.29
Ga*10000/A	2.3	1.9	1.7	2.0	2.2	2.1	2.0	2.0	2.0	1.9	2.2	2.3
Rb/Sr	0.3	1.1	1.8	2.3	2.3	1.4	1.3	0.6	0.6	0.7	0.9	2.8
Sr/Y	10.6	5.8	4.8	2.9	2.4	6.9	5.1	6.7	7.0	7.3	6.6	2.1
Zr-T(˚C)	784	743	703	716	714	752	729	741	729	739	773	738

Appendix: Continued.

	Seto zone								
	73	74	75	76	77	78	79	80	81
	65T84	65T94	65T92	65T90	65T89	65T96	66T70	65T86	66T145
SiO_2wt.%	74.33	73.75	74.71	75.76	75.22	74.96	75.87	76.20	75.56
TiO_2	0.20	0.18	0.18	0.11	0.16	0.14	0.09	0.10	0.09
Al_2O_3	13.00	13.23	12.74	12.45	12.94	13.03	12.80	12.57	12.84
Fe_2O_3	2.05	1.89	2.04	1.45	1.64	1.62	1.20	1.35	1.20
(FeO)	1.85	1.70	1.84	1.31	1.48	1.46	1.08	1.22	1.08
MnO	0.05	0.06	0.08	0.07	0.05	0.05	0.06	0.05	0.05
MgO	0.39	0.39	0.41	0.22	0.30	0.35	0.20	0.25	0.23
CaO	1.89	1.57	1.31	0.79	1.37	1.41	1.09	1.10	1.21
Na_2O	2.70	3.47	3.43	3.68	2.98	3.09	3.17	3.08	3.40
K_2O	4.54	4.35	4.47	4.83	4.85	4.74	4.84	4.67	4.50
P_2O_5	0.03	0.04	0.04	0.03	0.04	0.02	0.01	<0.01	<0.01
S	0.01	0.01	<0.01	<0.01	0.01	<0.01	0.01	<0.01	0.02
H_2O^+	0.63	0.82	0.43	0.49	0.28	0.66	0.38	0.49	0.45
H_2O^-	n.d.	0.16	n.d.	n.d.	n.d.	n.d.	0.24	n.d.	0.34
CO_2	n.d.	0.05	n.d.	n.d.	n.d.	n.d.	0.01	n.d.	0.04
Sum	99.82	99.96	99.84	99.86	99.83	100.06	99.96	99.85	99.91
Rb ppm	144	182	197	249	172	206	254	220	224
Cs	5.3	8.1	7.5	9.4	7.2	7.8	11.3	9.9	13.7
Sr	129	134	107	34	143	74	50	60	68
Ba	540	460	331	93	491	180	98	266	225
Zr	91	120	101	75	82	63	58	64	69
Hf	4	5.1	3.4	5.5	2.1	5.3	5.3	3.6	4.0
Nb	6.6	10.3	10	15.8	9	8.1	7.2	7.3	6.7
Ta	2.6	2.6	< 1.5	3.8	1.2	3.5	3.3	4.8	2.7
Y	28	42	31	52	23	52	62	32	28
La	27	31	31	12	28	11	33	20	15
Ce	57	55	57	30	51	25	33	36	26
V	13	15	16	6	14	<2	4	6	2
Cr	28	3	14	95	38	11	25	31	2
Co	7	9	5	6	5	9	7	6	8
Ni	2	<1	1	3	3	3	3	5	1
Cu	< 0.4	< 0.4	1	< 0.4	1	1	< 0.4	< 0.4	1
Zn	35	39	43	29	31	35	29	30	28
Pb	22	30	29	40	26	41	44	33	33
Ga	14.2	14.8	14.1	15	13.8	14.2	13.6	12.9	13.4
Ge	1.7	1.5	1.5	2	1.5	1.7	1.7	1.8	2.1
As	< 0.4	< 0.5	< 0.5	< 0.6	< 0.5	< 0.6	< 0.6	< 0.5	< 0.5
Se	0.2	0.1	0.1	< 0.1	< 0.1	0.2	0.2	< 0.1	0.1
Mo	0.6	0.2	0.3	0.5	1.9	0.5	0.5	0.6	< 0.2
W	< 0.9	1.4	0.9	3.6	1.5	2.3	2.3	2.1	0.4
Sn	1.8	4.8	5.3	5.6	2.7	4.6	4.5	4.2	5.9
Cd	< 0.2	< 0.2	< 0.2	< 0.2	< 0.2	0.2	< 0.2	0.3	< 0.2
Tl	1	1.2	1.5	1.6	1.4	1.7	1.6	1.6	1.4
Th	12.9	22.6	19.5	27.6	17.9	18.3	20.4	23.6	15.8
U	1.1	2.8	3	7.1	3.8	2.7	6.8	5	7.2
A/CNK	1.02	1.00	0.99	0.97	1.02	1.02	1.03	1.04	1.01
NK/A	0.72	0.79	0.82	0.91	0.78	0.78	0.82	0.80	0.82
Fe_2O_3/ MgO	5.21	4.88	5.02	6.73	5.48	4.65	6.05	5.43	5.18
Ga*10000/A	2.1	2.1	2.1	2.3	2.0	2.1	2.0	1.9	2.0
Rb/Sr	1.1	1.4	1.8	7.3	1.2	2.8	5.1	3.7	3.3
Sr/Y	4.6	3.2	3.5	0.7	6.2	1.4	0.8	1.9	2.4
Zr-T(˚C)	740	760	746	723	733	712	708	716	719